Launch Collision Probability

Gary Bollenbacher and James D. Guptill
Glenn Research Center, Cleveland, Ohio

National Aeronautics and
Space Administration

Glenn Research Center

Available from

Contents

Launch Collision Probability

Gary Bollenbacher and James D. Guptill
National Aeronautics and Space Administration
Glenn Research Center
Cleveland, Ohio 44135

Summary

This report analyzes the probability of a launch vehicle colliding with one of the nearly 10 000 tracked objects orbiting the Earth, given that an object on a near-collision course with the launch vehicle has been identified. Knowledge of the probability of collision throughout the launch window can be used to avoid launching at times when the probability of collision is unacceptably high. The analysis in this report assumes that the positions of the orbiting objects and the launch vehicle can be predicted as a function of time and therefore that any tracked object which comes close to the launch vehicle can be identified. The analysis further assumes that the position uncertainty of the launch vehicle and the approaching space object can be described with position covariance matrices. With these and some additional simplifying assumptions, a closed-form solution is developed using two approaches.

The solution shows that the probability of collision is a function of position uncertainties, the size of the two potentially colliding objects, and the nominal separation distance at the point of closest approach. The impact of the simplifying assumptions on the accuracy of the final result is assessed and the application of the results to the Cassini mission, launched in October 1997, is described. Other factors that affect the probability of collision are also discussed. Finally, the report offers alternative approaches that can be used to evaluate the probability of collision.

Introduction

Nearly 10 000 tracked objects are orbiting the Earth. These objects encompass manned objects, active and decommissioned satellites, spent rocket bodies, and debris. They range from a few centimeters in diameter to the size of the MIR Space Station. Their tracking and cataloging is the responsibility of the U.S. Air Force 1st Command and Control Squadron (CACS) at Cheyenne Mountain located in Colorado Springs, Colorado.

When a new satellite is launched, the launch vehicle with its payload attached passes through an area of space where these objects orbit. Although the object population density is low, there always exists a small but finite probability of collision between the launch vehicle and one or more space objects. Despite the very low probability of collision, even this small risk is unacceptable for some payloads, such as the Cassini spacecraft.

Cassini was launched by a Titan IV/Centaur rocket on an interplanetary trajectory at the window opening on October 15, 1997. The trajectory will take the Cassini spacecraft to Saturn via two Venus, an Earth, and a Jupiter gravity assists. It is a one-of-a kind, high-cost spacecraft equipped with three radioisotope thermoelectric generators fueled by 32.7 kg of the nonweapons grade isotope plutonium–238 dioxide. In addition, Cassini employs 117 lightweight radioisotope heater units, each containing 2.7 g of the same plutonium dioxide isotope. A collision with an orbiting space object would not only cause a loss of mission but would also risk the release of plutonium into the upper atmosphere.

To mitigate even the small risk of collision associated with launching at an arbitrary time within the daily launch window, a decision was made approximately 1 year before launch to require a collision avoidance analysis (COLA) that would be performed prior to the opening of each daily launch window. The analysis would examine the entire daily launch window and determine the launch times that resulted in an unacceptable potential for collision with any tracked object. Launch would not be attempted at any time for which an unacceptable potential for collision was identified. This mission assurance COLA, as it is sometimes called, was in addition to the safety COLA that is performed at the Eastern Range for all launches to protect orbiting manned objects or objects capable of being manned.

Mission assurance COLA analyses are routinely conducted by the Air Force for all Titan IV/Centaur launches. However, prior to the Cassini mission, the existing capability for COLA analyses was limited to the coast phases of a single, time-invariant trajectory, which was inadequate for the Cassini mission. The Cassini trajectory, unlike most Air Force missions, was a function of time into the window at which liftoff occurred. Additionally, the Cassini trajectory had a very long second Centaur burn, during which it passed through a region of space densely populated by space objects. To remedy these shortcomings, the Air Force developed new mission assurance COLA analysis software to satisfy NASA-defined requirements. These requirements were to perform a seamless COLA analysis from Titan stage II ignition up through geosynchronous altitude, including powered and coast flight phases, while fully accommodating the trajectory variability. The miss criteria used in the Air Force COLA analysis were developed by

NASA and were based on the probability analysis described in this report.

The variability of the Cassini trajectory is typical of interplanetary launches: it must link a nearly time-invariant interplanetary target (at the target planet) with a launch pad that is moving in space primarily as a result of the Earth's rotation. This is achieved by varying the direction of flight as a function of time into the window. The initial direction of flight is called the flight azimuth and is measured as the angle between the direction of flight and true north. For the Cassini mission, the variable flight azimuth was implemented as follows: The Titan stage 0 (the first stage) was designed to fly a planar trajectory of either 93° or 97° flight azimuth. The 93° flight azimuth was available from window opening until 80 min into the window; the 97° flight azimuth was allowed from 40 min into the window until window close, 140 min after window opening. Both azimuths were available between 40 and 80 min, selectable on launch day. Following stage 0, Titan stages 1 and 2 would perform yaw steering to place the launch vehicle into the astrodynamically correct flight plane. After jettisoning the Titan stage 2, the Centaur performed two planar main engine burns separated by a park-orbit coast. Both burn durations and the park-orbit coast duration were a function of liftoff time. Launch was planned to occur on the whole minute; thus, taking into account the two possible launch azimuths between 40 and 80 min into the 140-min launch window, there were 182 possible and different nominal launch trajectories for each day.

The software developed by the Air Force to perform COLA analysis for Cassini consisted of three parts:

1. Trajectory generator: For a given launch day, the trajectory generator creates a matrix of state vectors that accurately, though not perfectly, describe the position and velocity of the launch vehicle as a function of launch time, time into flight, and launch azimuth. State vectors for each of the 182 nominal trajectories required for each daily launch window are then passed on to the conjunction analyzer.

2. Conjunction analyzer: The conjunction analyzer compares the state vectors for each of the 182 trajectories for that day with the trajectories of all cataloged space objects. Any conjunction between the launch vehicle and a space object that violates predetermined criteria is identified and appropriate data are written to an output file that is then forwarded to the postprocessor.

3. Postprocessor: The postprocessor manipulates the data in the conjunction analyzer output file and generates easily readable summary charts that define unacceptable launch times. Prior to the opening of the launch window, these charts are distributed to the appropriate launch personnel.

NASA assumed the responsibility for specifying the criteria that were used in the conjunction analyzer. The criteria established a minimum clearance that was required between the launch vehicle and any space object. If, for any given liftoff time, the nominal launch vehicle trajectory passed a space object with less than the minimum required clearance, launch would not be attempted at that time in the window.

The miss distances computed by the conjunction analyzer are based on nominal trajectories. Four factors may cause the actual miss distances to differ substantially from the nominal miss distances computed by the conjunction analyzer:

1. Launch vehicle position uncertainties: Launch vehicle position errors, expressed as 3×3 position covariance matrices, will generally be a function of time from liftoff.

2. Space objects position uncertainties: Position errors of space objects are also given by 3×3 position covariance matrices that are generally a function of time since the last tracking.

3. Liftoff time errors: Errors in liftoff time occur because the resumption of the count at 5 min prior to liftoff is a manual operation and thus subject to operator reaction time. Errors in miss distance are the result of performing the COLA analysis for an assumed nominal liftoff time in the center of the tolerance range although the actual liftoff may occur earlier or later. Thus, the launch vehicle may arrive at some point in space earlier or later than nominal. With space objects traveling at rates up to 10 km/s, these liftoff time errors can have a substantial effect on actual miss distances.

4. Trajectory generation errors: As described above, the software developed by the Air Force reconstructed nominal launch vehicle trajectories. Although the methodology used by the trajectory generator is very accurate, it does introduce some small errors into the trajectories causing them to differ slightly from the planned trajectory.

The 3×3 covariance matrices describing the launch vehicle and the space object position uncertainties just discussed are generally based on normal distributions and this will be assumed throughout this report.

To establish appropriate miss criteria, NASA performed a probability analysis that defined the relationship of the nominal miss distance, the size of the objects, and the covariance matrices with the probability of collision. The miss distance requirement, based purely on probabilities, was then adjusted to account for liftoff time errors. Although there are a number of approaches that account for liftoff time errors, NASA selected a sufficiently conservative but simple methodology. This methodology justified omitting the small trajectory generation errors.

A final step in the establishment of miss criteria was to assess the reduction in launch window that would be lost because of miss criteria violations. A very conservative (large) miss criterion reduces the probability of collision but increases the number of unacceptable conjunctions, thereby potentially precluding launch during a significant portion of the launch window. Other than illustrating the resultant impact on the Cassini mission, the subject of launch availability will not be addressed further.

2

This report describes the analysis performed to assess the probability of collision. Two approaches are shown with each one requiring simplifying assumptions. The first approach is very intuitive and algebraically intensive. The second is mathematically more rigorous and offers the advantage of providing an estimate of the error introduced by the simplifying assumptions. Necessary adjustments due to the lack of adequate covariance data are also discussed. Finally, this report addresses other factors that must be considered in the establishment of the final miss criteria. The application of the results derived herein to the Cassini mission are described in appendix A. The symbols used are listed in appendix B.

Relative Motion Coordinate System

The probability analysis described in subsequent sections uses a relative motion coordinate system (RMCS), which is a reference system inertially fixed in space and defined at the moment of closest approach of the launch vehicle to a space object. As will be discussed in more detail later, the selection of this system makes the probability of collision independent of the z-direction, effectively reducing a three-dimensional problem to a two-dimensional one.

In the RMCS, the z-axis is in the direction of motion of one object relative to the other, the y-axis passes through both objects at the moment of closest approach, and the x-axis completes the orthogonal system shown in figure 1. As shown in the figure, the origin of the system is assumed to be at the center of one of the two conjuncting objects.

To compute the probability of collision, it will be necessary to transform the covariance matrices from inertial coordinates into the RMCS. The transformation can easily be derived if it
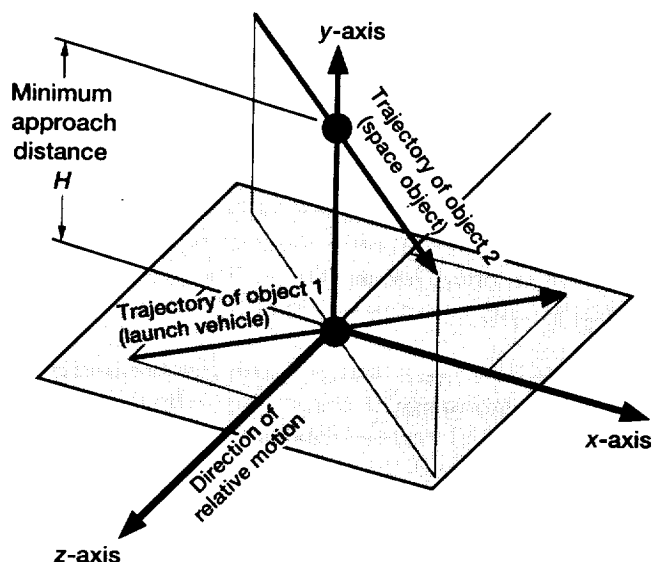
is assumed that the trajectory of both the launch vehicle and the conjuncting space object, while in proximity, can be represented as the motion along a straight line at a constant speed. For the purpose of this analysis, objects can be considered to be in proximity if there exists a probability of collision sufficiently large to be of concern. For all practical purposes, using the results derived in this report, probabilities of collision for nominal separation distances greater than ±100 km are negligible. Approximating any trajectory as a straight line over a distance of ±100 km from an arbitrary point along that trajectory is reasonable, for it can be shown that

1. For orbiting objects, a 200-km-long trajectory segment will deviate from a straight line tangent to the trajectory at its midpoint by no more than 0.8 km at the ends.
2. For the launch vehicle, based on an analysis of the Cassini trajectory, the maximum deviation from a 200-km-long straight line is 0.400 km.

Likewise, the assumption of constant velocity is valid, for it can be shown that the velocity change over the same ±100-km distance is

1. Less than 0.35 percent for orbiting objects
2. Less than 1.90 percent under worst-case conditions for a launch vehicle (based on an analysis of the Cassini trajectory); this worst-case velocity change occurs during Titan stage 2 burn, the first part of the trajectory; during Centaur main engine burns, the velocity change is less than 0.75 percent; and during coast phases it is less than 0.2 percent over the same distance.

Assume that for a given liftoff time, the position and the velocity of the launch vehicle and the space object can be expressed as a function of time from liftoff, referred to as mission elapsed time (MET). Given the assumption of linear motion at constant speed, the position vectors of the two objects as a function of time are written as

$$\mathbf{R}_{LV} = \left(a_{1,1} + b_{1,1}t\right)\mathbf{i} + \left(a_{1,2} + b_{1,2}t\right)\mathbf{j} + \left(a_{1,3} + b_{1,3}t\right)\mathbf{k}$$

$$\mathbf{R}_{SO} = \left(a_{2,1} + b_{2,1}t\right)\mathbf{i} + \left(a_{2,2} + b_{2,2}t\right)\mathbf{j} + \left(a_{2,3} + b_{2,3}t\right)\mathbf{k}$$

where $\mathbf{R}_{LV}$ and $\mathbf{R}_{SO}$ are the position vectors of the launch vehicle and the space object in inertial coordinates at time t; $a_{i,j}$ and $b_{i,j}$ are constants, and $\mathbf{i}$, $\mathbf{j}$, and $\mathbf{k}$ are orthogonal unit vectors in the inertial coordinate frame.

The difference between the two vectors, $\Delta\mathbf{R} = \mathbf{R}_{SO} - \mathbf{R}_{LV}$, is a vector that points from the launch vehicle to the space object and is expressed as

$$\Delta\mathbf{R} = \left(\tau_1 + \gamma_1 t\right)\mathbf{i} + \left(\tau_2 + \gamma_2 t\right)\mathbf{j} + \left(\tau_3 + \gamma_3 t\right)\mathbf{k} \qquad (1)$$

Figure 1.—Relative motion coordinate system (RMCS).

where $\tau_i = a_{2,i} - a_{1,i}$ and $\gamma_i = b_{2,i} - b_{1,i}$.

The time derivative of ΔR then gives the velocity of one object with respect to the other:

$$\frac{d(\Delta R)}{dt} = (\gamma_1)\mathbf{i} + (\gamma_2)\mathbf{j} + (\gamma_3)\mathbf{k}$$

The direction of this vector defines the z-direction of the RMCS. Note also that the relative velocity is along a fixed direction and has a constant magnitude.

At the point of closest approach, the first time derivative of the magnitude of ΔR must be zero:

$$\frac{d}{dt}|\Delta R| = 0$$

The time at which this derivative is zero, t_0, is given by

$$t_0 = \frac{-(\tau_1\gamma_1 + \tau_2\gamma_2 + \tau_3\gamma_3)}{\gamma_1^2 + \gamma_2^2 + \gamma_3^2}$$

Substituting this value of t_0 in equation (1) gives

$$\Delta R_{\text{closest approach}} = (\tau_1 + \gamma_1 t_0)\mathbf{i} + (\tau_2 + \gamma_2 t_0)\mathbf{j} + (\tau_3 + \gamma_3 t_0)\mathbf{k}$$

or more simply

$$\Delta R_{\text{closest approach}} = (\beta_1)\mathbf{i} + (\beta_2)\mathbf{j} + (\beta_3)\mathbf{k}$$

where the constants $\beta_i = \tau_i + \gamma_i t_0$. This vector defines the direction of the y-axis of the RMCS.

The direction of the x-axis of the RMCS is simply the crossproduct of $\Delta R_{\text{closest approach}}$ and $d(\Delta R)/dt$. The components of this vector will be designated α_1, α_2, and α_3.

The three orthogonal vectors defined by the components α_i, β_i, and γ_i are used to form the matrix

$$M = \begin{bmatrix} \alpha_1 & \alpha_2 & \alpha_3 \\ \beta_1 & \beta_2 & \beta_3 \\ \gamma_1 & \gamma_2 & \gamma_3 \end{bmatrix}$$

where it is now assumed that the rows of the matrix have been converted to unit magnitude.

Vectors and position covariance matrices are then easily transformed from inertial coordinates to the RMCS as follows:

$$V_{\text{RMCS}} = [M]V_{\text{Inertial}} \tag{2}$$

$$C_{\text{RMCS}} = [M][C_{\text{Inertial}}][M]^T \tag{3}$$

where V is any vector and C represents a 3×3 position covariance matrix.

In practice the equations of motion will not normally be expressed as equations of a straight line as assumed herein. Instead, a numerical integrator propagates the trajectory of the launch vehicle and the space object in small time increments. At each time step, R_{LV}, R_{SO}, and ΔR will be computed. The program will continuously monitor the separation distance ΔR to determine the point at which the magnitude of ΔR is minimum. The vector ΔR at that point defines the direction of the RMCS y-axis. By taking the values of ΔR at two different points in time near the point of closest approach, one can determine the direction of the RMCS z-axis. From these data, the values of α_i, β_i, and γ_i can be computed.

Probability of Collision

Approach 1

An expression for the probability of a launch vehicle collision with an orbiting space object is now derived. The assumptions are

1. An orbiting space object on a near-collision trajectory with the launch vehicle has been identified, and based on nominal trajectory propagation, the miss distance H has been determined; both objects are finite in size.

2. The velocity vector of one object relative to the other is constant (this is true if both objects move in a straight line at constant velocity as shown in the section Relative Motion Coordinate System).

3. A known position uncertainty of both objects exists relative to their nominal positions and these uncertainties are quantified by two 3×3 position covariance matrices.

4. The position errors are normally distributed; that is, covariance matrices are based on a normal multivariate distribution.

5. The covariance matrices are constant over the time interval when the two objects are in proximity.

6. The RMCS has been defined and all relevant quantities have been transformed into the RMCS. (This can be done, for example, by using equations (2) and (3).)

Even though the objects nominally approach one another no closer than H, the assumption of a position uncertainty implies that there exists some finite probability of collision. However, as will be demonstrated, the collision probability is independent of time and therefore of the position of the objects in the RMCS z-direction. Furthermore, it will be shown that the probability of collision does not depend on the position vari-

ances of either object in the z-direction or on any of the covariances that involve a component of z.

To establish the foregoing conclusions, consider the two objects as seen looking at the x,y-plane of the RMCS along a line parallel to the z-axis, as illustrated in figure 2. One of the two objects (it does not matter which) is assumed centered at the origin whereas the second object is nominally located on the y-axis a distance H from the first. In the z-direction, the objects are initially some distance apart. As object 2 moves with respect to object 1, the objects will become progressively closer until object 2 is at $z=0$, at which time the nominal separation distance is H. As object 2 continues to move in the z-direction, the separation distance will again increase.

The definition of the RMCS ensures that the velocity of object 2 relative to object 1 be entirely in the z-direction, with the velocity components in both the x- and y-directions being zero. Thus, the projection of the two objects into the x,y-plane is unaltered by the motion of object 2 relative to object 1.

To determine whether or not the objects will collide, one need only examine the location of the objects in the x,y-plane. When referring to the location of the objects, it is understood that reference is made to the position of just one point of each object designated as the object's "center" (although it need not be the true center). Given their finite sizes, both objects will also occupy some space surrounding the center. It is clear that a collision will result if any part of the projection into the x,y-plane of one object overlaps any part of the projection of the other object. To be more specific, if the two objects are located at their nominal position, as illustrated in figure 2, no collision will result. However, there is some probability that object 1 and object 2 are actually located at points x_1, y_1, and points x_2, y_2, respectively. The objects will collide if the separation between the two points x_1, y_1 and x_2, y_2 is less than the physical size of the objects.

The first step in the probability analysis is to determine the probability that object 1 is located at an arbitrary point x,y without regard to its location in the z-direction. To this end, let $p_1(x,y,z)$ be the three-dimensional probability density function associated with object 1. The function $p_1(x,y,z)$ is obtained by using the 3×3 covariance matrix of object 1 transformed into the RMCS. The two-dimensional probability function $p_1(x,y)$ is obtained by integrating the three-dimensional probability function $p(x,y,z)$ from $z = -\infty$ to $z = +\infty$:

$$p_1(x, y) = \int_{z=-\infty}^{z=+\infty} p_1(x, y, z)\,\mathrm{d}\,z$$

This integration can be performed under the assumption that the covariance matrices are not a function of time over the period of interest.

The function $p_1(x,y)$ is the density function associated with the marginal distribution of $p_1(x,y,z)$. By virtue of the normal
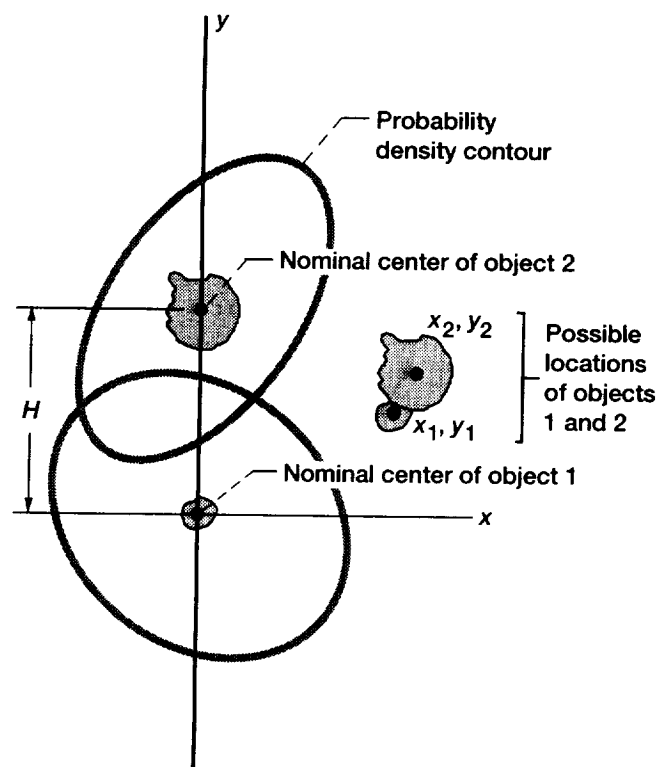
[1]Refer to Theorem 2.4.3, p. 31.

Figure 2.—Projection of two conjuncting objects into x, y-plane.

distribution assumption, it can be shown from reference 1[1] that the covariance matrix for the marginal distribution $p_1(x,y)$ is obtained from the original 3×3 covariance matrix by deleting the row and column corresponding to the z-direction to effectively remove the z-variance and the covariances involving position uncertainties in the z-direction. Thus, the marginal distribution $p_1(x,y)$ is only a function of variances and covariances involving x and y. When object 1 is located at point x_1, y_1, the probability density is then given by $p_1(x_1, y_1)$.

Similarly, when object 2 is located at point x,y, the probability density is given by $p_2(x,y)$, where the two-dimensional probability density of object 2 is obtained by using the three-dimensional covariance matrix for object 2 with the row and column corresponding to z deleted.

Return now to figure 2 and let the center of object 1 be located at some point x_1, y_1. If the center of object 2 is also located at point x_1, y_1, the two objects will collide. However, given the finite size of both objects, they will also collide if the center of object 2 is some distance removed from object 1. In fact, there are many points where the center of object 2 can be located such that a collision of the two objects will result. For example, consider the case in which the cross-sectional area of both objects when projected in the x,y-plane is a circle, as illustrated in figure 3. The first object is centered at x_1, y_1. If the center of the second object is anywhere within the dashed circle, the

Integrate probability density function of object 2 over region R^* bounded by this circle
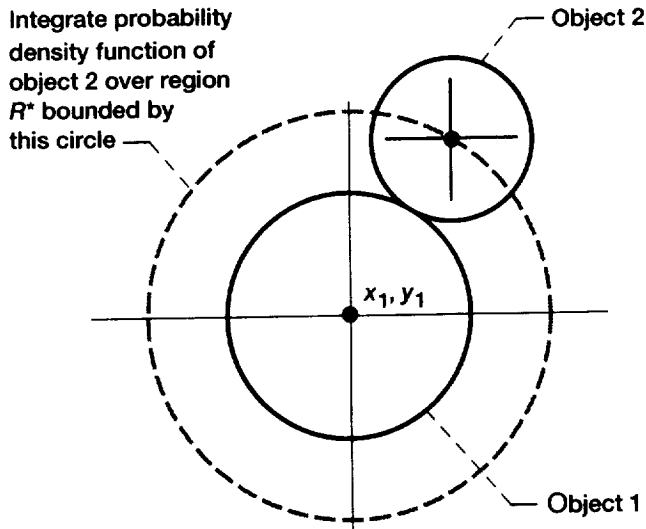
Object 2

x_1, y_1

Object 1

Figure 3.—Illustration of region R^* for objects with circular cross sections.

two objects will collide. The two-dimensional region bounded by the dashed circle is designated R^*, the area of which is A^*.

In actuality, the cross-sectional areas presented to the x, y-plane will not be circles. Furthermore, the shape, size, and orientation of the cross-sectional areas will generally not be known. Nevertheless, there will exist for any two objects a region R^* such that if the center of object 2 is within that region, a collision will result.

Thus, given probability density p_1 when object 1 is located at x_1, y_1, the collision probability density is

$$p = p_1(x_1, y_1) \int_{R^*} p_2(x, y) \, dA \qquad (4)$$

where the integration is carried out over the region R^*.

At this point an assumption will be made to greatly simplify the remainder of the derivation. This assumption will have the effect of degrading the accuracy of the final result, particularly for large values of A^*. This effect will be quantified in a later section of this report. The simplifying assumption is to let the probability density function $p_2(x, y)$ at an arbitrary point x, y be constant over the region R^* and be equal to its value at point x_1, y_1, that is

$$p_2(x, y) = p_2(x_1, y_1)$$

for all points x, y within the region R^*. With this assumption, given that object 1 is located at x_1, y_1, the collision probability density given in equation (4) can be rewritten as

$$p \approx p_C = p_1(x_1, y_1) p_2(x_1, y_1) A^*$$

To obtain the overall probability of collision, integrate over all possible locations of object 1, with the resultant probability of collision being

$$P_C = \int_{y_1 = -\infty}^{y_1 = +\infty} \int_{x_1 = -\infty}^{x_1 = +\infty} p_C \, dx_1 \, dy_1$$

$$P_C = A^* \int_{y_1 = -\infty}^{y_1 = +\infty} \int_{x_1 = -\infty}^{x_1 = +\infty} \left[p_1(x_1, y_1) p_2(x_1, y_1) \right] dx_1 \, dy_1 \qquad (5)$$

Since the two covariance matrices are assumed to be known, it is possible to expand the probability density functions and explicitly perform the two integrations to arrive at a closed-form solution for the probability of collision. This procedure is now described.

Assume that the two-dimensional covariance matrix for object 1 is given by

$$\begin{bmatrix} \sigma_1^2 & \rho_1 \sigma_1 v_1 \\ \rho_1 \sigma_1 v_1 & v_1^2 \end{bmatrix}$$

where σ_1 and v_1 are the 1-sigma position uncertainties along the x- and y-directions, respectively, and ρ_1 is the correlation between the x- and y-errors. This matrix is the original 3×3 covariance matrix for object 1 in the RMCS with the row and column corresponding to the z-direction deleted. Similarly, let

$$\begin{bmatrix} \sigma_2^2 & \rho_2 \sigma_2 v_2 \\ \rho_2 \sigma_2 v_2 & v_2^2 \end{bmatrix}$$

be the covariance matrix for object 2. The corresponding probability density functions are then given by

$$p_1 = \frac{1}{2\pi \sigma_1 v_1 \sqrt{1 - \rho_1^2}}$$

$$\times e^{\frac{-1}{2(1 - \rho_1^2)} \left[(x/\sigma_1)^2 - 2\rho_1 (x/\sigma_1)(y/v_1) + (y/v_1)^2 \right]}$$

and

$$p_2 = \frac{1}{2\pi \sigma_2 v_2 \sqrt{1 - \rho_2^2}}$$

$$\times e^{\frac{-1}{2(1 - \rho_2^2)} \left\{ (x/\sigma_2)^2 - 2\rho_2 (x/\sigma_2)[(y-H)/v_2] + [(y-H)/v_2]^2 \right\}}$$

These equations assume that the distributions associated with p_1 and p_2 have means of (0,0) and (0,H), respectively.

When these expressions for the probability density function are substituted into equation (5) and the indicated multiplication carried out, the resultant expression can then be integrated by successively applying the following integration formula (ref. 2)[2]

$$\int_{-\infty}^{+\infty} e^{-\left(ax^2+bx+c\right)} \, dx = \sqrt{\frac{\pi}{a}} \, e^{\left(b^2-4ac\right)/4a} \qquad (6)$$

First the integration formula is applied to the inner integration with respect to x_1 to obtain

$$P_C = A^* \frac{\sqrt{a_1 a_2}}{2\pi^2} \sqrt{\frac{\pi}{b_1}} \int_{y_1=-\infty}^{y_1=+\infty} \left[e^{\left(b_2^2-4b_1 b_3\right)/4b_1} \right] dy_1$$

where

$$a_1 = \frac{1}{2\left(1-\rho_1^2\right)\sigma_1^2 v_1^2}$$

$$a_2 = \frac{1}{2\left(1-\rho_2^2\right)\sigma_2^2 v_2^2}$$

$$b_1 = a_1 v_1^2 + a_2 v_2^2$$

$$b_2 = -2\left[a_1\rho_1\sigma_1 v_1 y_1 + a_2\rho_2\sigma_2 v_2 (y_1 - H)\right]$$

$$b_3 = a_1\sigma_1^2 y_1^2 + a_2\sigma_2^2 (y_1 - H)^2$$

This can be rewritten as

$$P_C = A^* \frac{\sqrt{a_1 a_2}}{2\pi^2} \sqrt{\frac{\pi}{b_1}} \int_{y_1=-\infty}^{y_1=+\infty} \left[e^{-\left(F_1 y_1^2 + F_2 y_1 + F_3\right)} \right] dy_1$$

where

$$F_1 = \frac{a_1^2\left(1-\rho_1^2\right)\sigma_1^2 v_1^2 + a_2^2\left(1-\rho_2^2\right)\sigma_2^2 v_2^2 + a_1 a_2\left(\sigma_1^2 v_2^2 + \sigma_2^2 v_1^2 - 2\rho_1\rho_2\sigma_1\sigma_2 v_1 v_2\right)}{\left(a_1 v_1^2 + a_2 v_2^2\right)}$$

$$F_2 = -2H \frac{a_2^2\sigma_2^2 v_2^2\left(1-\rho_2^2\right) + a_1 a_2\left(\sigma_2^2 v_1^2 - \rho_1\rho_2\sigma_1\sigma_2 v_1 v_2\right)}{\left(a_1 v_1^2 + a_2 v_2^2\right)}$$

$$F_3 = \left(H\sigma_2\right)^2 \frac{a_2^2 v_2^2\left(1-\rho_2^2\right) + a_1 a_2 v_1^2}{\left(a_1 v_1^2 + a_2 v_2^2\right)}$$

Again, applying equation (6) to the integration with respect to y_1 yields

$$P_C = A^* \frac{\sqrt{a_1 a_2}}{2\pi^2} \sqrt{\frac{\pi}{b_1}} \sqrt{\frac{\pi}{F_1}} \, e^{\left(F_2^2-4F_1 F_3\right)/4F_1}$$

Making obvious substitutions and after a great deal of tedious algebra, the result is

$$P_C = \frac{A^*}{2\pi} \frac{1}{\sqrt{\left(\sigma_1^2+\sigma_2^2\right)\left(v_1^2+v_2^2\right)-\left(\rho_1\sigma_1 v_1+\rho_2\sigma_2 v_2\right)^2}}$$

$$\times e^{-0.5\left\{\left(\sigma_1^2+\sigma_2^2\right)/\left[\left(\sigma_1^2+\sigma_2^2\right)\left(v_1^2+v_2^2\right)-\left(\rho_1\sigma_1 v_1+\rho_2\sigma_2 v_2\right)^2\right]\right\}H^2}$$

$$(7)$$

This can be simplified by defining a new covariance matrix Σ, which is simply the sum of the two individual covariance matrices:

$$\Sigma = \begin{bmatrix} \sigma_T^2 & \rho_T\sigma_T v_T \\ \rho_T\sigma_T v_T & v_T^2 \end{bmatrix}$$

$$= \begin{bmatrix} \sigma_1^2 & \rho_1\sigma_1 v_1 \\ \rho_1\sigma_1 v_1 & v_1^2 \end{bmatrix} + \begin{bmatrix} \sigma_2^2 & \rho_2\sigma_2 v_2 \\ \rho_2\sigma_2 v_2 & v_2^2 \end{bmatrix} \qquad (8)$$

and substituting the new covariance terms into equation (7)

---

[2]Table 15, formula 15.75, p. 98.

$$P_C = \frac{A^*}{2\pi} \frac{1}{\sqrt{(\sigma_T)^2(v_T)^2 - (\rho_T \sigma_T v_T)^2}}$$

$$\times e^{-0.5\left\{(\sigma_T)^2 / \left[(\sigma_T)^2(v_T)^2 - (\rho_T \sigma_T v_T)^2\right]\right\} H^2}$$

or

$$P_C = \frac{A^*}{2\pi} \frac{1}{\sigma_T v_T \sqrt{1 - \rho_T^2}} e^{-0.5 H^2 / \left[v_T^2(1 - \rho_T^2)\right]}$$

One more simplification is possible by letting

$$v_{eqv} = v_T \sqrt{1 - \rho_T^2}$$

where v_{eqv} is an equivalent position error in the y-direction with zero correlation, and the final result then becomes

$$P_C = \left(\frac{A^*}{2\pi}\right)\left(\frac{1}{\sigma_T v_{eqv}}\right) e^{-0.5\left(H^2 / v_{eqv}^2\right)} \tag{9}$$

The next section will provide an alternative approach for deriving equation (9), which additionally yields a basis for estimating the errors inherent in equation (9) because of the assumption made during its derivation.

Approach 2

This section provides another way to model the probability of collision to utilize some of the power of a rigorous mathematical approach and to present the basis on which to evaluate the effect of the simplifying assumption highlighted in approach 1. In particular, for each object, a vector of three random variables associated with the x,y,z-coordinates of the object in the RMCS will be defined. These variables are then combined and transformed (using the eigenvalues and eigenvectors of the covariance matrix) to produce two random variables that are independent and are associated with one-dimensional standard normal distributions (with means 0 and variances 1).

Because of the mathematical formalism used in this section, it is useful to review the definition of random variable and to see how the definition is applied to near-collision trajectories. Random variable is defined (ref. 3)[3] as a mapping (or function) from an event space to a number on the number line. A classical example is rolling a pair of dice where the event is the roll itself (i.e., one roll out of the event space of all possible rolls). The random variable provides a recipe for extracting a number from

any such event. In the case of rolling dice, the recipe (or mapping) involves counting the dots facing up on the two dice. In this paper, the event space includes all possible trajectories (i.e., those related to all possible position uncertainties) of the two objects (launch vehicle and orbiting object) associated with one identified near-collision trajectory. From this event space, the actual positions of the two objects at the moment of nominally closest approach can be extracted. For example, one mapping (random variable) can be defined from the event space to the real number line by identifying the x-coordinate (in the RMCS) of the location of object 1 at the time of closest approach. Similarly, five more mappings can be defined for the y- and z-coordinates of object 1 and for all three coordinates of object 2. To distinguish between real numbers and random variables, this section uses upper case letters for random variables, upper case letters with arrows for vectors (or ordered sets) of random variables, and lower case letters for real numbers.

The same six assumptions listed at the beginning of the section Approach 1 are also made here. Let the random variable $\vec{E}$ map a trajectory event to the ordered triple of coordinates associated with the location in the RMCS of the center of object 1 at the moment of nominally closest approach. Similarly, let the random variable $\vec{F}$ map to the coordinates of the location of the center of object 2. Then, $\vec{E}$ and $\vec{F}$ are distributed as trivariate normal distributions with means $(0,0,0)$ and $(0,H,0)$ and, say, covariances $\Sigma_E^{(3)}$ and $\Sigma_F^{(3)}$, respectively.

In this approach, the two three-dimensional random variables are combined first and then a marginal distribution is extracted. In a way similar to the earlier discussion but in reference to all three dimensions, a collision is defined to occur when the two objects are positioned such that any part of one object occupies the same volume as any part of the other object. In particular, the location of the two objects *relative to each other* completely determines whether or not a collision occurs irrespective of where the pair of objects is located in space. (Note this differs from the first approach for modeling the probability of collision wherein the location of one object was fixed at some (albeit arbitrary) point, the coordinates of which are later used as a dummy variable of integration.) Then a three-dimensional region S^* can be defined based on the *relative* positions of the two objects at the time of nominally closest approach such that whenever the relative positions are "near enough to each other" to be inside S^*, the two objects will collide. To define the relative location of the two objects with respect to each other, subtract the two position vectors associated with the two objects. Moreover, define a mapping from a trajectory event to a set of three coordinates in the RMCS of this relative location vector by a new random variable $\vec{G} = \vec{F} - \vec{E}$. Note that this effectively reduces the dimensionality of the problem from six (three coordinates for each of two objects) to three components of the relative position vector. Although $\vec{G}$

---

[3]Definition 1, p. 53.

8

maps events to a somewhat different vector space from that of the other two random variables, its components are referred to as X,Y,Z. Note that the region of collision S^* is centered at the origin of the $\bar{G}$-space (i.e., when $\bar{E} = \bar{F}$). In a manner similar to the discussion in the first approach but now in three dimensions, consider a case in which both objects are spheres. The region S^* is also a sphere centered at the origin with a radius equal to the sum of the radii of the two objects. Clearly, the projection of S^* into the x,y-plane is just a circle. In particular, it is the region R^* identified in the first approach but translated from x_1,y_1 to the origin of the $\bar{G}$-space. This relationship between S^* and R^* will hold no matter what the shapes of the two objects. Call this new region R_0^*, which is the same as R^* but is translated to the origin of $\bar{G}$-space. The area of R_0^* is A^* as before.

Now, assume that $\bar{E}$ and $\bar{F}$ are independent; that is, assume that information about the location of one object does not provide information about the location of the other object. With the independence assumption, it can be shown (ref. 1)[4] that $\bar{G}$ is distributed as a trivariate normal random variable with mean $(0,H,0)$ and covariance $\Sigma^{(3)} = \Sigma_E^{(3)} + \Sigma_F^{(3)}$.

Next, recall that the z-direction is parallel to the relative velocity vector of the objects; thus, the variance in the z-direction corresponds to delays in the arrival of or the premature arrival of object 1 *relative to* object 2 at some point on the x,y-plane passing through the origin of the RMCS. The desire is to determine the probability of collision irrespective of the time of collision (i.e., a collision occurs whether it happens early or late in the near-collision trajectory). Thus, the marginal distribution of $\bar{G}$ is taken by integrating out the random variable associated with movement in the z-direction. The covariance of this marginal distribution is obtained by deleting the row and column associated with movement in the z-direction (ref. 1)[5]. Thus, using the notation given in equation (8) of the first approach, the associated random variable is a bivariate normal with mean $(0,H)$ and covariance matrix

$$\Sigma = \begin{bmatrix} \sigma_T^2 & \rho_T \sigma_T v_T \\ \rho_T \sigma_T v_T & v_T^2 \end{bmatrix}$$

Note that the variances do not address liftoff time errors, which will be discussed in the section Application of Results to Collision Avoidance (COLA) Analysis.

The probability of collision can be found by integrating the two-dimensional probability density function of this bivariate normal distribution $p_{XY}(x,y)$, for example, over the region R_0^* centered at the origin as noted earlier:

[4]Refer to Theorem 2.4.4, p. 31. In Anderson's notation, take Σ to be the 6×6 covariance matrix composed of $\Sigma_E^{(3)}$ as the upper left submatrix, $\Sigma_F^{(3)}$ in the lower right, and two 3×3 zero matrices elsewhere (due to the independence of $\bar{E}$ and $\bar{F}$), take μ to be $(0,0,0,0,H,0)$, and take D to be the 3×6 matrix $[-I\ I]$, where I is the 3×3 identity matrix.

[5]Refer to Theorem 2.4.3, p. 31.

$$P = \int_{R_0^*} p_{XY}(x,y)\,dA$$

where $p_{XY}(x,y)$ is the probability density function associated with Σ and is given by

$$p_{XY}(x,y) = \frac{1}{2\pi\sigma_T v_T \sqrt{1-\rho_T^2}}$$

$$\times e^{\frac{-1}{2(1-\rho_T^2)}\left\{(x/\sigma_T)^2 - 2\rho_T(x/\sigma_T)[(y-H)/v_T] + [(y-H)/v_T]^2\right\}}$$

For comparison, consider applying the simplifying assumption taken in the first approach. In $\bar{G}$-space the equivalent assumption is that the probability density is constant over the region of integration R_0^* centered at the origin and is equal to its value at this origin. Substituting $(0,0)$ for (x,y), the integral reduces to

$$P_C = \int_{R_0^*} p_{XY}(0,0)\,dA$$

$$= p_{XY}(0,0) \int_{R_0^*} dA$$

$$= A^* \frac{1}{2\pi\sigma_T v_T \sqrt{1-\rho_T^2}} e^{-0.5 H^2 / \left[v_T^2\left(1-\rho_T^2\right)\right]}$$

or simplifying,

$$P_C = \left(\frac{A^*}{2\pi}\right)\left(\frac{1}{\sigma_T v_{eqv}}\right) e^{-0.5\left(H^2 / v_{eqv}^2\right)} \tag{9}$$

which is the same result obtained previously.

This same formula can also be reproduced without the assumption that the probability density is constant in the region of integration; rather, it can be assumed that

(a) The region R_0^* is a rectangle whose sides are parallel to the major and minor axes of the probability density contour associated with the covariance matrix Σ.

(b) A Taylor series expansion can be performed on the resultant expression with only the first term retained.

The remainder of this section is devoted to deriving a more precise formula for the rectangular region and then approximating the more precise formula with the first term in its Taylor expansion. A following section will examine the error resulting from dropping all but the first term of the Taylor expansion.

Starting in $\bar{G}$-space and using a standard technique (ref. 4)[6], the random variables X and Y can be transformed into two independent standard normal random variables, U and V. This technique depends on several facts, one of which is that the covariance matrix is symmetric. Another is that for any symmetric matrix, an orthonormal matrix N exists such that $N^T \Sigma N = K$ where K is a diagonal matrix with elements that are the (real) eigenvalues (ref. 5)[7] of Σ. Using the positive definiteness of the covariance matrix (ref. 1)[8], the eigenvalues are positive (ref. 5)[9] so their square roots are real. Thus, a real diagonal matrix D can be formed, the elements of which are the square roots of the eigenvalues of Σ. In particular, U and V are independent standard normal random variables if they are defined by the transformation of variables (ref. 4)[10]

$$\begin{bmatrix} U \\ V \end{bmatrix} = D^{-1} N^T \left(\begin{bmatrix} X \\ Y \end{bmatrix} - \begin{bmatrix} 0 \\ H \end{bmatrix} \right) \tag{10}$$

where N is an orthonormal matrix with columns that are the normalized eigenvectors of Σ, and D is a diagonal matrix with elements that are the square roots of the corresponding eigenvalues. The variables U and V resulting from this transformation are dimensionless. Using this transformation, the probability of collision becomes

$$P = \int\limits_{R'} p_U(u) p_V(v) \, d\,u\,d\,v \tag{11a}$$

where

$$p_U(u) = \frac{1}{\sqrt{2\pi}} e^{-0.5u^2} \tag{11b}$$

$$p_V(v) = \frac{1}{\sqrt{2\pi}} e^{-0.5v^2} \tag{11c}$$

and R' is the region obtained by translating the region R_0^* by $(0, -H)$, rotating it by N^T, and rescaling it by D^{-1}. Note here that the eigenvalues are given by

$$\lambda_{\pm} = \frac{\sigma_T^2 + v_T^2 \pm \sqrt{\left(\sigma_T^2 - v_T^2 \right)^2 + 4\rho_T^2 \sigma_T^2 v_T^2}}{2} \tag{12}$$

Since matrix multiplication by the two-dimensional orthonormal matrix N simply rotates a region without changing its size, the area A^* of the original region is unmodified under both

translation and rotation; however, it is changed by a factor of $|D^{-1}|$ during rescaling. Thus, using the eigenvalues defined above, the area A' of the transformed region R' after a little algebra, becomes

$$A' = A^* |D^{-1}|$$

$$= \frac{A^*}{\sqrt{\lambda_+ \lambda_-}}$$

$$= A^* \frac{1}{\sigma_T v_T \sqrt{1 - \rho_T^2}}$$

The derivation up to now is applicable to a region R_0^* of any size or shape. However, the integration indicated in equation (11a) is difficult to carry out analytically for an arbitrarily shaped region. To enable the evaluation of the integral, the above derivation is now applied to a rectangular-shaped region centered at the origin of the $\bar{G}$-space in the RMCS with sides parallel to the major and minor axes of the elliptical density contours associated with the covariance matrix, as illustrated in figure 4.

Here, θ is the angle of orientation of both the rectangle and the elliptical density contour with respect to the x-axis. In the following, it is assumed that $-\pi/4 < \theta \leq \pi/4$; L^* is the length of the sides of the rectangular R_0^* which are oriented in the direction of θ; and W^* is the length of the other sides. Note that L^* may or may not be larger than W^*.
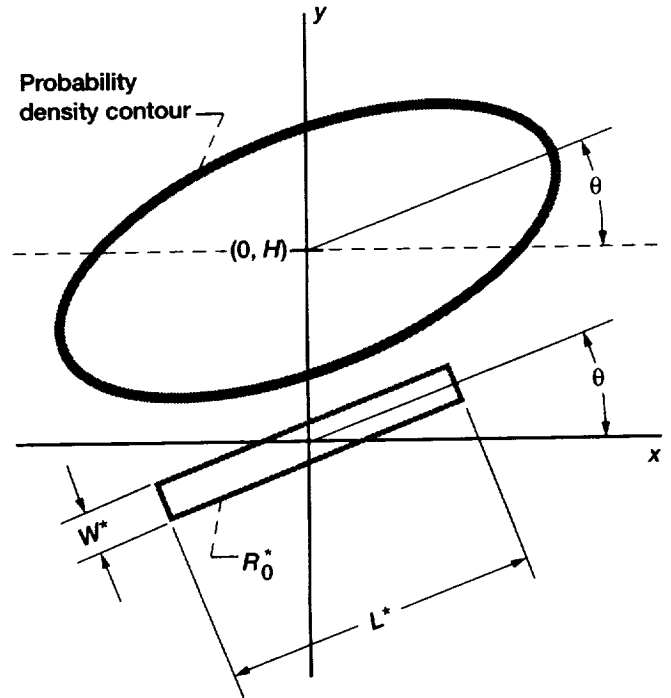

Figure 4.—Rectangular region R_0^* in x, y-plane.

---

[6]Section 3.1, p. 49.
[7]Section 23, p. 26.
[8]Section 2.3, p. 14.
[9]Section 26, p. 28.
[10]Section 3.1, p. 49.

10

It is further assumed that $\sigma_T^2 > v_T^2$, in which case the following are true:

(1) θ defines the orientation of the major axis of the density contour with respect to the x-axis.

(2) L^* is defined in direction θ (i.e., parallel to the major axis of the density contour).

(3) λ_+ is associated with the axis of the density contour that lies in the θ-direction (i.e., the major axis).

If $v_T^2 > \sigma_T^2$, then replace "major" with "minor" in the discussion below, since the following are true:

(1) θ defines the orientation of the minor axis of the density contour with respect to the x-axis.

(2) L^* is defined in direction θ (i.e., parallel to the minor axis of the density contour).

(3) λ_+ is to be associated with the axis of the density contour that lies in the θ-direction (i.e., the minor axis), in which case the $\pm$ in equation (12) for the eigenvalues must be replaced with $\mp$.

The angle θ is given by the following relationship, which can be derived from the definition of the contours of the density function p_{XY}:

$$\tan 2\theta = \frac{2\rho_T \sigma_T v_T}{\sigma_T^2 - v_T^2} \tag{13}$$

Use this equation to write the eigenvalues as

$$\lambda_\pm = \frac{\sigma_T^2 + v_T^2}{2} \pm \frac{\sigma_T^2 - v_T^2}{2}\sqrt{1 + \tan^2 2\theta}$$

$$= \frac{\sigma_T^2 + v_T^2}{2} \pm \frac{\sigma_T^2 - v_T^2}{2\cos 2\theta} \tag{14}$$

Substituting the expressions for the eigenvalues given in equation (14) into the characteristic (or eigen-) equation will provide the eigenvectors. Using the eigenvectors as the columns of the matrix N and using equation (13) along with a few trigonometric identities, the matrix N can be simplified to obtain

$$N = \begin{bmatrix} \cos\theta & -\sin\theta \\ \sin\theta & \cos\theta \end{bmatrix}$$

Then after translating the region R_0^* by $(0,-H)$ and rotating by N^T, the rectangle will have sides parallel to the u- and v-axes. The rescaled region R' of length L' and W' centered at a point we shall call (u',v') is illustrated in figure 5. Note that
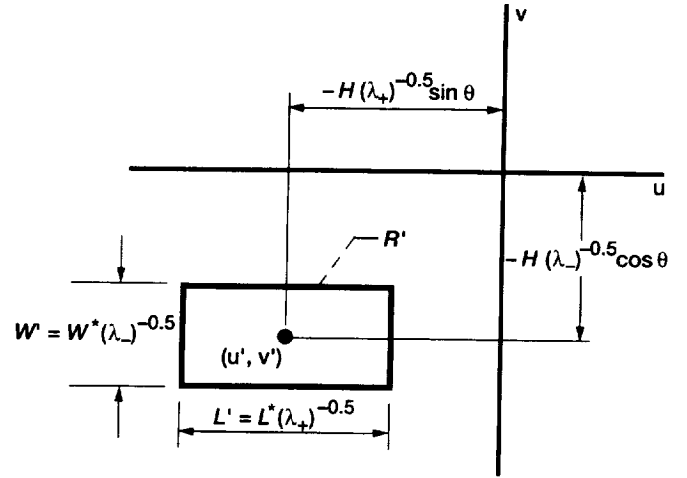
Figure 5.—Rectangular region R' in u, v-plane.

$$L'W' = A'$$

$$= A^* \frac{1}{\sigma_T v_T \sqrt{1 - \rho_T^2}}$$

$$= \frac{L^* W^*}{\sigma_T v_T \sqrt{1 - \rho_T^2}} \tag{15}$$

Note, also, that neither the translation nor the rotation of R_0^* described above will change its dimensions, but rescaling will modify the dimension parallel to the u-axis by the first element of D^{-1} and the dimension parallel to the v-axis by the second element of D^{-1}. In particular,

$$L' = \frac{L^*}{\sqrt{\lambda_+}} \tag{16a}$$

$$W' = \frac{W^*}{\sqrt{\lambda_-}} \tag{16b}$$

It should also be pointed out that $\sqrt{\lambda_+}$ and $\sqrt{\lambda_-}$ are the lengths of the semimajor and semiminor (or semiminor and semimajor) axes of a particular probability density contour associated with the covariance matrix Σ. Thus, L' and W' are nondimensional quantities, the ratios of the lengths of the sides of the rectangular region R_0^* to the lengths of the semimajor and semiminor axes of a probability density contour of Σ.

The probability of collision for this region can now be easily found. Since U and V are independent and the region of integration is a rectangle whose sides are parallel to the u- and v-axes, the required probability is the product of two one-dimensional probabilities. Each of these probabilities, in turn, is obtained by taking the difference of their cumulative distribution functions evaluated at the upper and lower limits of the region. In particular,

$$P = \left[P_U(u' + 0.5L') - P_U(u' - 0.5L') \right]$$
$$\times \left[P_V(v' + 0.5W') - P_V(v' - 0.5W') \right] \qquad (17)$$

where $P_U(u)$ and $P_V(v)$ are the one-dimensional cumulative distribution functions for the standard normal distribution given by

$$P_U(u) = \int_{-\infty}^{u} p_U(\gamma)\, d\gamma$$

$$P_V(v) = \int_{-\infty}^{v} p_V(\gamma)\, d\gamma \qquad (18)$$

where p_U and p_V are the one-dimensional standard normal density functions defined in equations (11b) and (11c).

Noting that commercial software is available for quickly calculating the one-dimensional cumulative distribution function for a standard normal distribution and that the simplifying assumption highlighted in the first approach was not taken to derive this formula for the probability of collision, it might seem desirable to use this formula directly. However, recall that this formula is only good for the particular circumstance in which the region R_0^* is a rectangle with sides parallel to the major and minor axes of the probability contours associated with Σ.

In the final portion of this section, the first term of the Taylor expansion of the formula for P given in equation (17) will be examined and rewritten to obtain again the formula derived in the first approach (eq. (9)) for calculating the probability of collision. In the next section, the remainder term of the Taylor expansion will be used to compare these two approaches.

Consider the first multiplicand in equation (17). Expanding P_U in a Taylor series about the point u' and evaluating at $u' + 0.5L'$ and $u' - 0.5L'$ gives

$$P_U(u' + 0.5L') = P_U(u') + \frac{d\,P_U}{d\,u}\bigg|_{u'} (0.5L')$$
$$+ \frac{1}{2!}\frac{d^2\,P_U}{d\,u^2}\bigg|_{u'} (0.5L')^2 + \dots \qquad (19a)$$

$$P_U(u' - 0.5L') = P_U(u') - \frac{d\,P_U}{d\,u}\bigg|_{u'} (0.5L')$$
$$+ \frac{1}{2!}\frac{d^2\,P_U}{d\,u^2}\bigg|_{u'} (0.5L')^2 + \dots \qquad (19b)$$

Subtracting the two Taylor series gives

$$P_U(u' + 0.5L') - P_U(u' - 0.5L') = \frac{d\,P_U}{d\,u}\bigg|_{u'} (L') + \dots$$

Proceeding in a similar way for the second multiplicand, dropping higher order terms, and substituting into equation (17) provides

$$P \approx \left(\frac{d\,P_U}{d\,u}\bigg|_{u=u'} \right)(L')\left(\frac{d\,P_V}{d\,v}\bigg|_{v=v'} \right)(W') \qquad (20)$$

or

$$P \approx L'W'p_U(u')p_V(v')$$

since the derivative of the cumulative distribution function is just the probability density function (ref. 3)[11]. This is the same result one would obtain by integrating the probability density functions p_U and p_V over the rectangle R' and by assuming that the probability density functions are constant at their value at u', v', which is consistent with the assumption made in the first approach.

Substituting u' and v' into the probability density functions given by equations (11b) and (11c) and using the relationship between $L'W'$ and L^*W^* of equation (15)

$$P \approx \frac{L^*W^*}{\sigma_T v_T \sqrt{1 - \rho_T^2}} \frac{1}{2\pi} e^{-0.5(u'^2 + v'^2)} \qquad (21)$$

Next, u' and v' are replaced by the components of the original covariance matrix Σ. To find (u', v') using the transformation of variables from the X,Y-space to the U,V-space given earlier by equation (10), translate the center of the region R_0^* (i.e., the origin) by $(0,-H)$, rotate by N^T and rescale by D^{-1} to obtain

$$\begin{bmatrix} u' \\ v' \end{bmatrix} = -H \begin{bmatrix} \dfrac{\sin\theta}{\sqrt{\lambda_+}} \\ \dfrac{\cos\theta}{\sqrt{\lambda_-}} \end{bmatrix} \qquad (22)$$

---

[11]Theorem 2, p. 61.

Thus

$$u'^2 + v'^2 = H^2 \left(\frac{\lambda_- \sin^2 \theta + \lambda_+ \cos^2 \theta}{\lambda_+ \lambda_-} \right)$$

Using equation (14) for the eigenvalues, the numerator reduces, after some algebra, to simply σ_T^2. Substituting in the original expressions for the eigenvalues, equation (12), in the denominator, after a little more algebra, gives

$$u'^2 + v'^2 = \frac{H^2}{v_T^2 \left(1 - \rho_T^2\right)}$$

Finally, substituting the above into equation (21) gives

$$P \approx \frac{L^* W^*}{\sigma_T v_T \sqrt{1 - \rho_T^2}} \frac{1}{2\pi} e^{-0.5\, H^2 / \left[v_T^2 \left(1 - \rho_T^2\right) \right]}$$

$$\approx \left(\frac{A^*}{2\pi} \right) \left(\frac{1}{\sigma_T v_{eqv}} \right) e^{-0.5 \left(H^2 / v_{eqv}^2 \right)}$$

The last term will be recognized as the value of P_C derived previously, leading to the conclusion that

$$P \approx P_C = \left(\frac{A^*}{2\pi} \right) \left(\frac{1}{\sigma_T v_{eqv}} \right) e^{-0.5 \left(H^2 / v_{eqv}^2 \right)} \qquad (23)$$

Thus, P_C is the first term of the Taylor series expansion of the more precise formula given in equation (17) when applied to a rectangular region R_0^*.

As demonstrated in this and in the previous section, the probability of collision shown in equations (9) and (23) applies to either (1) an arbitrarily shaped region of area A^*, provided that one can assume that p_C is constant over the region R^*, or (2) a rectangular region of area A^* with its sides aligned with the major and minor axes of the error ellipsoids, provided that one can assume that the higher order terms of the Taylor expansion are negligible. The next section evaluates the higher order terms of the Taylor series expansion to arrive at an estimate of the error introduced in the equation for P_C by the simplifying assumptions made in approaches 1 and 2.

Accuracy of Probability Equation

This section provides information to clarify the magnitude of the error associated with neglecting the higher order terms of the Taylor series expansion. This error is the same as that which results from assuming a constant probability density over the

region R^*, R_0^*, or R'. In general this error will be a function of the shape and orientation of the region. However, even though equation (9) is valid for an arbitrarily shaped region, the error will be examined for the case of a rectangular region R_0^* with sides parallel to the major and minor axes of the probability contours. In particular, the more precise formula of equation (17) derived in approach 2 is approximated by a Taylor expansion, and the remainder terms are examined. The remainder terms are shown to depend on the area A^* of the regions R_0^* or R^*.

The more precise formula derived in approach 2 is

$$P = \left[P_U(u' + 0.5L') - P_U(u' - 0.5L') \right]$$
$$\times \left[P_V(v' + 0.5W') - P_V(v' - 0.5W') \right] \qquad (17)$$

where, from equations (16) and (22),

$$u' = -H \frac{\sin \theta}{\sqrt{\lambda_+}}; \quad v' = -H \frac{\cos \theta}{\sqrt{\lambda_-}}; \quad L' = \frac{L^*}{\sqrt{\lambda_+}}; \quad W' = \frac{W^*}{\sqrt{\lambda_-}}$$

and H is the nominal miss distance between the orbiting space object and the launch vehicle at the moment of closest approach, L^* and W^* are the lengths of the rectangular region R_0^*, and $P_U(u)$ and $P_V(v)$ are the one-dimensional cumulative distribution functions for the standard normal distribution given in equation (18).

As before, consider a series representation of the first multiplicand in the formula above, but this time focus on the higher order terms. First, expanding P_U in a Taylor series about the point u' and evaluating at $u' + 0.5L'$ and $u' - 0.5L'$ gives (as before in equation (19))

$$P_U(u' + 0.5L') = P_U(u')$$
$$+ \left. \frac{d P_U}{d u} \right|_{u'} (0.5L') + \frac{1}{2!} \left. \frac{d^2 P_U}{du^2} \right|_{u'} (0.5L')^2 + R_{3+}$$

$$P_U(u' - 0.5L') = P_U(u')$$
$$- \left. \frac{d P_U}{d u} \right|_{u'} (0.5L') + \frac{1}{2!} \left. \frac{d^2 P_U}{du^2} \right|_{u'} (0.5L')^2 + R_{3-}$$

where using Lagrange's form of the remainder (ref. 2)[12] gives

$$R_{3+} = \frac{1}{3!} \left. \frac{d^3 P_U}{d^3 u} \right|_{\tilde{u}} (0.5L')^3, \quad \text{for some } \tilde{u} \ni u' \leq \tilde{u} \leq u' + 0.5L'$$

---

[12]Table 20, formulas 20.1 and 20.2, p. 110.

$$R_{3-} = -\frac{1}{3!} \left.\frac{d^3 P_U}{d^3 u}\right|_{\tilde{u}} (0.5L')^3, \text{ for some } \tilde{u} \ni u' - 0.5L' \le \tilde{u} \le u'$$

Subtracting the two truncated Taylor series gives

$$P_U(u' + 0.5L') - P_U(u' - 0.5L') = \left.\frac{d P_U}{d u}\right|_{u'} (L') + R_U$$

where $R_U = R_{3+} - R_{3-}$.
To estimate the remainder term R_U, note that

$$|R_U| \le |R_{3+}| + |R_{3-}|$$

$$\le \frac{1}{3!} M_+ (0.5L')^3 + \frac{1}{3!} M_- (0.5L')^3$$

$$= \frac{1}{48}(M_+ + M_-)(L')^3$$

where M_+ and M_- are defined such that

$$\left|\frac{d^3 P_U}{d u^3}\right| \le M_+ \quad \forall u \ni u' \le u \le u' + 0.5L'$$

$$\left|\frac{d^3 P_U}{d u^3}\right| \le M_- \quad \forall u \ni u' - 0.5L' \le u \le u'$$

To estimate M_+ and M_-, recall that the derivative of P_U is the probability density function p_U. Thus,

$$\frac{d^2 P_U}{d u^2} = \frac{d p_U}{d u}$$

$$= -\frac{u}{\sqrt{2\pi}} e^{-0.5u^2}$$

$$\frac{d^3 P_U}{d u^3} = \frac{u^2 - 1}{\sqrt{2\pi}} e^{-0.5u^2}$$

The third derivative is shown in figure 6. Note that the maximum of the absolute value of the third derivative of P_U occurs at $u = 0$ and has a value of $(2\pi)^{-0.5}$, or 0.399. Using this conservative value for M_+ and M_- will be sufficient for the discussion here. (If the entire interval of length L' centered at u' lies more than four units away from the origin, the values of M_+ and M_- and the error terms become very much smaller.) Substituting $(2\pi)^{-0.5}$ for M_+ and M_- gives
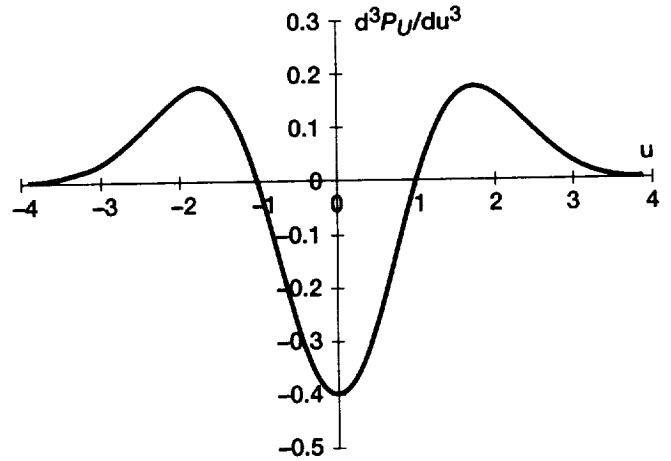
Figure 6.—Third derivative of standard normal cumulative distribution function, P_U.

$$|R_U| \le \frac{1}{24\sqrt{2\pi}} L'^3 \tag{24}$$

The same procedure can be carried out for the second multiplicand in equation (17) to obtain

$$P_V(v' + 0.5W') - P_V(v' - 0.5W') = \left.\frac{d P_V}{d v}\right|_{v'} (W') + R_V$$

where

$$|R_V| \le \frac{1}{24\sqrt{2\pi}} W'^3 \tag{25}$$

Substituting into equation (17) produces

$$P = \left(\left.\frac{d P_U}{d u}\right|_{u'} L' + R_U\right)\left(\left.\frac{d P_V}{d v}\right|_{v'} W' + R_V\right)$$

$$= \left(\left.\frac{d P_U}{d u}\right|_{u'}\right)\left(\left.\frac{d P_V}{d v}\right|_{v'}\right) L'W'$$

$$+ \left(\left.\frac{d P_V}{d v}\right|_{v'}\right) R_U W' + \left(\left.\frac{d P_U}{d u}\right|_{u'}\right) R_V L' + R_U R_V$$

This equation can be reduced to

$$P = P_C + R_T$$

by recognizing that the first term is P_C from equations (20) and (23), where R_T consists of the three remainder terms and can be bounded for any u´, v´, L´, and W´ by noting that

$$\left|\frac{d\,P_U}{d\,u}\right| \leq \frac{1}{\sqrt{2\pi}}; \quad \left|\frac{d\,P_V}{d\,v}\right| \leq \frac{1}{\sqrt{2\pi}} \quad \forall\ u, v \qquad (26)$$

Then

$$|R_T| \leq \left|\left(\frac{d\,P_V}{d\,v}\bigg|_{v'}\right)\right| |R_U||W'| + \left|\left(\frac{d\,P_U}{d\,u}\bigg|_{u'}\right)\right| |R_V||L'| + |R_U||R_V|$$

$$\leq \frac{1}{\sqrt{2\pi}}\frac{1}{24\sqrt{2\pi}}L'^3 W' + \frac{1}{\sqrt{2\pi}}\frac{1}{24\sqrt{2\pi}}L'W'^3$$

$$+ \frac{1}{24\sqrt{2\pi}}\frac{1}{24\sqrt{2\pi}}L'^3 W'^3$$

$$= \frac{1}{48\pi}(L'W')L'^2 + \frac{1}{48\pi}(L'W')W'^2$$

$$+ \frac{1}{1152\pi}(L'W')^3 \qquad (27)$$

To examine these remainder terms, note that the area of the probability density contour defined by

$$[x \quad y]\Sigma^{-1}\begin{bmatrix} x \\ y \end{bmatrix} = 1 \qquad (28)$$

can be written as

$$A^\sigma = \pi\sqrt{\lambda_+}\sqrt{\lambda_-} \qquad (29)$$

Thus,

$$L'W' = \frac{L^*W^*}{\sqrt{\lambda_+}\sqrt{\lambda_-}} = \pi\frac{A^*}{A^\sigma} \qquad (30)$$

That is, $L'W'$ is proportional to the ratio of the area A^* of the region R^* to the area of the probability density contour defined by equation (28). Finally, substituting into equation (27),

$$|R_T| \leq \frac{1}{48}\frac{A^*}{A^\sigma}\left(L'^2 + W'^2\right) + \frac{\pi^2}{1152}\left(\frac{A^*}{A^\sigma}\right)^3$$

or

$$|R_T| \leq \frac{1}{48}\frac{A^*}{A^\sigma}\left(\frac{L^{*2}}{\lambda_+} + \frac{W^{*2}}{\lambda_-}\right) + \frac{\pi^2}{1152}\left(\frac{A^*}{A^\sigma}\right)^3 \qquad (31)$$

Equation (31) provides an upper bound for the absolute value of the error produced by any one of the following:

(1) Truncating the Taylor series expansion of equation (17)

(2) Assuming a constant probability density $p_U p_V$ whose value is taken at the center of R' (see eq. (20))

(3) Assuming a constant probability density function p_2 whose value is taken at the center of R^* (see eq. (4))

In all cases, the bound is valid only when the regions R' (or R_0^*) or R^* are rectangular and properly aligned.

The following observations can be made regarding equation (31) for the error term $|R_T|$:

(1) All terms are functions of the ratio of the physical size of the two colliding objects to the size of the probability density contour associated with the covariance matrix Σ.

(2) For cases in which the two terms inside the first parentheses are approximately equal, this sum could be replaced with twice $L'W'$ or by applying equation (30), with 2π times the ratio of the areas A^* to A^σ, thus providing an error bound that depends only on this area ratio.

(3) The error bound is not a function of the separation distance H because of the conservative assumptions made in the derivation of $|R_T|$ in equations (24) to (26). In particular, eliminating the dependency of $|R_T|$ on u´ and v´ removed the dependency on H.

(4) Terms A^σ and λ_- (or λ_+ if $v_T^2 > \sigma_T^2$) are zero when the correlation ρ_T of the covariance matrix Σ becomes 1.0. In this case, the bound for the error R_T becomes infinite. However, as is shown in appendix A, for values of $\rho_T \leq 0.95$, the error R_T is very small.

In addition, it can be shown that if the rectangular region R_0^* is oriented such that the long side of the rectangle is parallel to the minor axis of the density contour, the error bound will be larger than that obtained if the long side is parallel to the major axis of the density contour. This alignment occurs if $L^* < W^*$ and $\lambda_+ > \lambda_-$, or if $L^* > W^*$ and $\lambda_+ < \lambda_-$.

The bound for the remainder term can be rewritten in terms of the elements of Σ (σ_T, v_T, and ρ_T) to obtain

$$|R_r| \leq \left(\frac{A^*}{2\pi}\right)\left(\frac{1}{\sigma_T v_{eqv}}\right)$$

$$\times \left[\frac{\left(L'^2 + W'^2\right)\left(\sigma_T^2 + v_T^2\right) - \left(L'^2 - W'^2\right)\sqrt{\left(\sigma_T^2 - v_T^2\right)^2 + 4\rho_T^2\sigma_T^2 v_T^2}}{48\sigma_T^2 v_{eqv}^2}\right]$$

$$+ \frac{1}{1152\pi}\left(\frac{A^{*3}}{\sigma_T^3 v_{eqv}^3}\right)$$

Note that if ρ_T is 1, then $v_{eqv} = 0$.

One final note in this section should be made. The estimate for the remainder term given herein can be quite conservative. A better estimate can sometimes be obtained when the values of u', L', v', and W' allow utilizing less conservative estimates for

$$|R_U|, \quad |R_V|, \quad \left|\frac{d P_U}{d u}\right|, \quad \text{and} \quad \left|\frac{d P_V}{d v}\right|$$

In these cases, the error becomes a function of the minimum separation distance H.

Discussion of Results

Using two different approaches has shown that the probability of collision of two objects is given by

$$P_C = \left(\frac{A^*}{2\pi}\right)\left(\frac{1}{\sigma_T v_{eqv}}\right)e^{-0.5\left(H^2/v_{eqv}^2\right)} \tag{9}$$

where

$$v_{eqv} = v_T\sqrt{1 - \rho_T^2}$$

and the variables are defined as follows:

v_T combined position error in y-direction
σ_T combined position error in x-direction
ρ_T correlation of combined covariance matrix
A^* area of a composite region, centered at one object such that if center of second object is within that region, a collision results
H nominal separation distance of two objects at point of closest approach

The area A^* needs some additional explanation. To begin with, A^* is a function of the actual cross-sectional areas and the shape of the colliding objects as they are projected into the x,y-plane, which in turn is a function of the actual object sizes and their orientations relative to the RMCS reference frame. In practice, the actual object sizes are not always known and certainly the orientations of the objects are unknown. At best, what is known is the radar cross section of the objects and the object type (satellite, rocket body, or debris) from which some information about the object size can be deduced. However, even if the sizes and shapes of the objects in the x,y-plane are known, there remains the question of how to compute A^*. To shed some light on this, consider first the situation in which both objects present a circular cross section to the x,y-plane as shown in figure 3. If the circular cross-sections are of area A_1 and A_2 and of radius r_1 and r_2, respectively, then

$$A^* = \pi\left(r_1 + r_2\right)^2$$
$$= A_1 + A_2 + 2\sqrt{A_1 A_2}$$
$$= \left(\sqrt{A_1} + \sqrt{A_2}\right)^2$$

Similarly, if both objects project as squares with areas A_1 and A_2 and sides of length l_1 and l_2, respectively, then

$$A^* = \left(l_1 + l_2\right)^2$$
$$= A_1 + A_2 + 2\sqrt{A_1 A_2}$$
$$= \left(\sqrt{A_1} + \sqrt{A_2}\right)^2$$

For rectangles, the situation is slightly more complicated. Consider two rectangles whose sides are parallel to the x- and y-axes. Let a_1 and a_2 be the lengths of the two rectangles in the x-direction and b_1 and b_2 be the lengths of the rectangles in the y-direction. Further let

$$A_1 = \left(a_1\right)\left(b_1\right)$$
$$A_2 = \left(a_2\right)\left(b_2\right)$$
$$k_1 = \frac{a_1}{b_1}$$
$$k_2 = \frac{a_2}{b_2}$$

16

Then

$$A^* = A_1 + A_2 + \left(\frac{k_1 + k_2}{\sqrt{k_1 k_2}} \right) \sqrt{A_1 A_2}$$

The minimum value of the factor $(k_1 + k_2)/\sqrt{k_1 k_2}$ is 2, which is the case when $k_1 = k_2$; that is, when the two rectangles have the same aspect ratio. A special case of this is when $k_1 = k_2 = 1$, in which both rectangles are squares. When the two constants are not equal, the above factor is mathematically unbounded. In reality, assuming plausible aspect ratios, the factor can easily become much larger than 2. Thus, for two rectangles at least, it is seen that A^* is always larger than $\left(\sqrt{A_1} + \sqrt{A_2} \right)^2$, which is always larger than the sum of the two areas and depending on the shapes of the two rectangles, can become quite large.

Similar calculations for other simple shapes have been made and the resultant area A^* has always been found to be equal to or larger than $\left(\sqrt{A_1} + \sqrt{A_2} \right)^2$.

Next, the expression for the probability of collision is examined in greater detail. The probability of collision is illustrated in figure 7, which graphs P_C as a function of H using the values $A^* = 500 \, \text{m}^2$, $\sigma_T = 2 \, \text{km}$, and v_{eqv} is represented parametrically from 1 to 20 km.

From an examination of equation (9) and figure 7, the following conclusions can be drawn:

(1) The value of P_C is directly proportional to A^* and is inversely proportional to σ_T.

(2) The value of P_C declines monotonically with increasing values of H.

(3) The term P_C is a function of the combined covariance matrix of objects 1 and 2 only.

(4) The value of v_{eqv} that results in the highest probability of collision when $H = 0$ results in the lowest probability of collision as H increases.

(5) The probability of collision falls off most rapidly with increasing H for small values of v_{eqv}.

By differentiating the expression for P_C with respect to v_{eqv} and equating the result to zero (providing that $v_{eqv} \neq 0$ and $H \neq 0$), it is easily seen that the maximum probability of collision occurs when $v_{eqv} = H$. Substituting H for v_{eqv} then yields the maximum probability of collision:

$$(P_C)_{max} = \frac{e^{-0.5}}{2\pi} \frac{A^*}{\sigma_T H} \tag{32}$$

Thus, it is seen that the maximum probability of collision depends only on the values of A^*, σ_T, and H, where $H = v_{eqv} > 0$.

Returning to equation (9), if $H = 0$, then the probability of collision is

$$(P_C)_{H=0} = \frac{1}{2\pi} \frac{A^*}{\sigma_T v_{eqv}}$$

This equation shows that if two large objects (e.g., A^* is 2000 m^2) are nominally on a collision course ($H = 0$) and the combined one-sigma position errors in the x- and y-directions are both only 0.5 km, then the probability of collision is still less than 13 in 10 000.
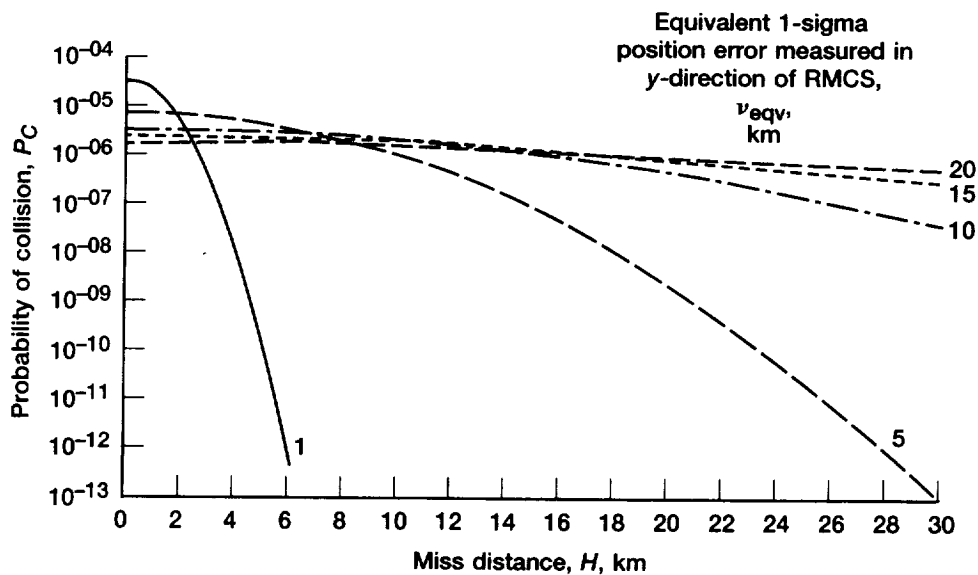

Figure 7.—Probability of collision P_C versus miss distance H. Area of region R^*, A^*, 500 m^2; 1-sigma position error measured in x-direction of RMCS, σ_T, 2 km.

Application of Results to Collision Avoidance (COLA) Analysis

To use the probability of collision equation to perform a COLA analysis, ideally this procedure would be followed:

(1) Propagate the trajectories of a space object and the launch vehicle to the point of closest approach based on an assumed launch vehicle liftoff time.

(2) Determine the nominal closest approach distance H.

(3) Compute the transformation matrix M to convert from the coordinate system used for the state vector propagation into the RMCS.

(4) Determine the covariance matrices of both objects at the time of closest approach.

(5) Transform the covariance matrices associated with both conjuncting objects into the RMCS.

(6) Reduce the 3×3 covariance matrices to 2×2 covariance matrices by deleting the row and column corresponding to the z-direction.

(7) Add the two covariance matrices to determine σ_T and v_{eqv}.

(8) Compute or assume a value for the area A^* by assuming some knowledge of the type of space object in close conjunction with the launch vehicle.

(9) Use equation (9) to compute the probability of collision.

(10) If the probability of collision is larger than some predetermined threshold value, launch would not be attempted at the liftoff time assumed in step 1.

One modification to this procedure may be necessary. As was mentioned previously, liftoff may not occur at the exact time assumed in step 1 because of a tolerance that may be as large as several seconds. Any error in the liftoff time results in the launch vehicle arriving at a specific point in space either early or late. With space objects potentially traveling at a velocity of 10 km/s, the actual miss distance could be substantially less than that computed in step 2. Some methods for dealing with this problem follow:

(1) Reduce the miss distance H as computed in step 2 by the worst-case distance that a space object could travel if launch occurred at the extreme ends of the tolerance range. For example, if the tolerance is ±2 s and the maximum space object velocity is 10 km/s, reduce the computed H by 20 km. This is equivalent to the approach taken for Cassini as described in more detail in appendix A.

(2) Use method 1 but instead of assuming that the velocity of the space object is 10 km/s, assume the worst-case velocity at the altitude of the conjunction. With this method, H would be reduced by a lesser amount for conjunctions that occur at higher altitudes.

(3) Perform a COLA analysis over small time increments covering the entire liftoff time tolerance range. If the probability criterion were to be violated at any time within the tolerance

range, no launch attempt would be made at the corresponding nominal liftoff time.

The preceding discussion assumes that the covariance matrices for both objects are known. The next section discusses a procedure that can be used if one or both covariance matrices are not known.

Collision Avoidance Analysis With Unknown Covariance Matrices

When the covariance matrix for one or both of the objects is unknown, the procedure for calculating the probability of collision, as given in the previous section, is not possible and a different approach is suggested. This section shows that it is possible to determine a minimum miss distance which will ensure that the probability of collision is less than some desired value regardless of the position errors or correlations of either object.

The first step in this analysis is to solve equation (9) for H, yielding the following result:

$$H_{min} = \sqrt{\left(-2.0 v_{eqv}^2\right)\left[\ln\left(\frac{2\pi P_C \sigma_T v_{eqv}}{A^*}\right)\right]} \qquad (33)$$

For any given covariance matrix, this equation gives the minimum nominal separation distance H_{min} required for any specified value of P_C. If the nominal separation distance is greater than H_{min}, the probability of collision will be less than P_C.

Equation (33) is shown graphically in figure 8 using the following numeric values: $P_C = 1.0 \times 10^{-6}$, $A^* = 500$ m^2, and σ_T parametrically from 2 to 10 km. Each curve in the figure represents the variation of H_{min} as a function of v_{eqv} for a constant value of σ_T. Note that for a constant σ_T, as v_{eqv} is increased the separation distance required to maintain a probability of collision of $P_C = 1.0 \times 10^{-6}$ first rises, reaches a maximum, and then declines again. This maximum separation distance is designated H_{max} and by differentiating equation (33) with respect to v_{eqv} is found to be

$$H_{max} = e^{-0.5} \frac{A^*}{2\pi \sigma_T P_C}$$

This is the same as equation (32) for $(P_C)_{max}$ derived earlier, only with the terms rearranged. The value of v_{eqv} that gives the maximum value of H_{max} is designated v_{max} and, recalling from before, is equal to H_{max}:

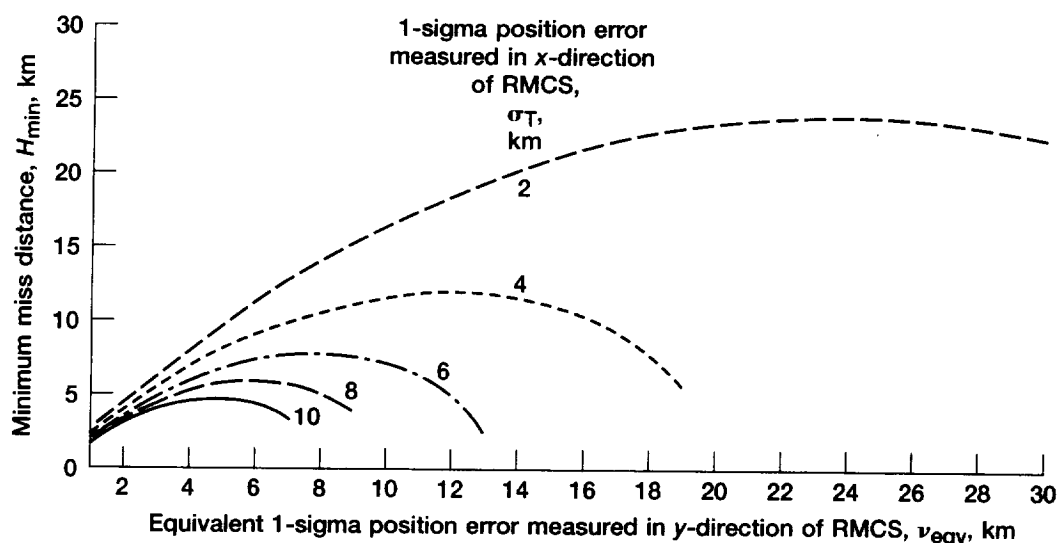$$v_{max} = H_{max} = e^{-0.5} \frac{A^*}{2\pi \sigma_T P_C} \qquad (34)$$

Figure 8.—Minimum required miss distance H. Probability of collision P_C, 1.0×10^{-6}; area of region R^*, A^*, 500 m^2.

Thus, if v_{eqv} of the combined covariance matrices of objects 1 and 2 is unknown, one can assume that $v_{eqv} = v_{max}$. The required minimum separation distance to ensure that the probability of collision be less than P_C is H_{max}. The computation of H_{max} still requires knowledge of the value of σ_T. Under worst-case assumptions, the absolute largest separation distance required would be the value of H_{max} when σ_T assumes its smallest possible value σ_{min}. This value is designated H^*:

$$H^* = e^{-0.5} \frac{A^*}{2\pi\sigma_{min}P_C} \tag{35}$$

As long as the separation distance between the launch vehicle and any space object is greater than H^*, the probability of collision will always be less than P_C regardless of the values of the launch vehicle or the space object covariance matrices. In fact, the only time that the probability of collision will be equal to P_C is when $v_{eqv} = v_{max}$ and $\sigma_T = \sigma_{min}$. Using this procedure, the only knowledge required of the two covariance matrices is the value of σ_{min}.

For Cassini (see appendix A for detailed description), the value of σ_{min} was estimated, maximum values of A^* were computed for several classes of orbiting objects, and a criterion for P_C was established. Based on these values, the absolute largest required nominal separation distance H^* was computed for each class of orbiting objects. Liftoff would not have been attempted anytime that the COLA analysis revealed a violation of the required miss distance H^*.

Alternative Approaches to Computing Probability

The foregoing sections illustrate the usefulness of deriving an analytical expression for the probability of collision and the

insights that can be gained by examination of that expression. An alternative might be to calculate the probability of collision numerically, as alluded to near the end of the section Probability of Collision, Approach 2. Recall that equation (17) gave the probability of collision formula that would allow the use of commercial software for calculating the one-dimensional cumulative distribution function for a standard normal distribution. It has the advantage of not requiring the simplification highlighted in the first approach to modeling that probability of collision, but it does require that the region R_0^* be rectangular and oriented in the same direction as the probability density contour of the covariance matrix.

Several steps are required to use this alternative approach. The first is to establish the rectangle discussed immediately above. If the region R_0^* is not already rectangular, a rectangle meeting all the criteria can be formed to be large enough to encompass all the true region R_0^*. This would be a conservative approach because the probability obtained would be larger (possibly much larger) than the probability that the objects would come close enough to be within the true region R_0^*.

The next step is to calculate the eigenvalues using equation (12) or (14) and to obtain the angle of orientation θ using equation (13). Then u', v', L', and W' can be calculated using equations (22) and (16). Finally, the four values of the cumulative distribution function can be found and combined to obtain the (conservative) probability of collision.

The authors wish to suggest an additional approach that would not be burdened by the requirement of a rectangular region R_0^* but would have a more involved setup and would be more computationally expensive. Such an approach would require the transformation of the (now arbitrary) region R_0^* to R' either using the transformation from the x,y-plane to the u,v-plane given in equation (10) to obtain the region R' parametrically (if R_0^* is given explicitly or parametrically) or using the inverse of

that transformation to obtain R' implicitly (if R_0^* is given implicitly). Then, one must integrate (perhaps numerically) the product of two standard normal density functions (for which commercial software is available) over the region R'. Note that the transformation referred to herein also requires the calculation of the angle θ and the eigenvalues.

Summary of Results

A model is presented for the determination of the probability of collision between a launch vehicle/payload combination and any one of the many tracked objects orbiting the Earth. The model was specifically developed for the Cassini mission (launched in October 1997) but is clearly applicable to other launches. It consists of a closed-form solution that shows the effect each of the independent parameters has on the probability of collision. The model can be applied to compute the probability of collision throughout a daily launch window and thereby afford the opportunity to avoid launching at those times within that window when the probability of collision is unacceptably high. For a given maximum probability of collision and prior knowledge of the objects' position uncertainties, only knowledge of the nominal closest approach distance is required to make this launch/no launch decision.

Two approaches are presented for deriving this model. One uses a practical engineering approach and the other, a more mathematically rigorous approach. Each uses different but equivalent simplifying assumptions, presents the material from different points of view, and produces the same simplified model. Using the second approach results in the development of an expression for the magnitude of the error introduced by the simplifying assumption.

The simplified model developed by both approaches expresses the probability of collision as a function of

(1) A composite area related to the size of the two objects
(2) The position covariance matrices of both objects
(3) The nominal separation distance measured at the point of closest approach

More specifically, the simplified model for the probability of collision is shown to be

$$P_C = \left(\frac{A^*}{2\pi}\right)\left(\frac{1}{\sigma_T v_{eqv}}\right)e^{-0.5\left(H^2/v_{eqv}^2\right)} \qquad (9)$$

where

$$v_{eqv} = v_T\sqrt{1 - \rho_T^2}$$

and the variables are defined as follows:

A^* area of region centered at one object such that if the center of the second object is within the region, a collision results

σ_T^2, v_T^2 variances in the RMCS x- and y-directions of covariance matrix obtained by adding the position covariance matrices of the launch vehicle and orbiting object at the point of nominally closest approach and eliminating the row and column associated with the z-direction

ρ_T correlation coefficient of this combined 2×2 covariance matrix

H nominal separation distance of two objects at the point of closest approach

Further analysis allows the model to be used in cases when the covariance matrices (and therefore σ_T, v_T, and ρ_T) are not completely known and involves the computation of a minimum required separation distance under worst-case assumptions regarding the two-position covariance matrices. This modified approach assures that as long as the nominal separation distance is greater than the minimum required, an allowable probability of collision will not be exceeded.

The application of these results to the Cassini mission is provided in appendix A, which also discusses some other factors that must be considered and addresses the impact on the available launch window of limiting the probability of collision. Using Cassini data, an estimate of the error in this equation resulting from the simplifying assumption of both approaches suggests that the model is acceptable for most launches.

Appendix A

Application of Probability Analysis to Cassini Mission

The analysis developed in this report was applied to the COLA analysis for the Cassini mission. Detailed descriptions of how the miss criteria were developed and their effect on the launch window are described. Also presented are data for all identified conjunctions that violated the miss criteria for the actual day of launch. The discussion concludes with an assessment of the accuracy of the probability analysis.

For the Cassini mission, accurate, reliable covariance matrices for orbiting space objects were not available. This situation required that the approach to be used for COLA analysis when covariance matrices are not known was that presented in the section Collision Avoidance Analysis With Unknown Covariance Matrices. The launch/no launch decision was made by comparing the nominal miss distance H to criteria that were determined weeks before launch. If the distance from the launch vehicle to all space objects exceeded the miss criteria, the launch could proceed.

A severe schedule constraint dictated that the development of miss criteria rely heavily on making worst-case assumptions rather than on attempting to refine the accuracy of the data used. Initially some concern was that the use of worst-case assumptions would lead to miss criteria so large that the launch availability would be severely impacted; therefore, to maintain launch availability, it was necessary to increase the maximum allowed probability of collision from 1.0×10^{-6} to 1.0×10^{-5}. It is safe to state however, that although the miss criteria were based on a probability of collision of 1.0×10^{-5}, the numerous worst-case assumptions that were made resulted in a considerably lower actual probability of collision.

Development of Miss Criteria

In the absence of covariance data, the miss distance was computed by using

$$H^* = e^{-0.5} \frac{A^*}{2\pi\sigma_{min}P_C} \tag{35}$$

or

$$H^* = 0.09653 \frac{A^*}{\sigma_{min}P_C} \tag{36}$$

and by adjusting the results for a number of factors, including the worst-case liftoff time error.

Three items had to be determined to calculate the miss distance: (1) the value of σ_{min}, (2) suitable values of A^*, and (3) the largest acceptable collision probability P_C.

Selecting a value of σ_{min}.—To determine the value of σ_{min}, the conservative approach was to assume that

$$\sigma_{min} = min(\sigma_1) + min(\sigma_2)$$

The best accuracy with which the position of space objects is known depends on several factors, including the type of orbit the object is in and the radar cross section of the object. Air Force personnel estimated that the position error for some space objects could be as low as 200 to 300 m. Assuming that this position error was in the x-direction of the RMCS frame led to the conclusion that min (σ_1) was 200 m.

To determine the smallest position error for the launch vehicle, an error analysis was performed for a typical Cassini trajectory. The analysis computed covariance matrices at fixed times throughout the trajectory. Eigenvalues, the square root of which represents the position errors, were computed for each covariance matrix and the smallest eigenvalue at each time point was selected. Examination of these data revealed that the best position accuracy was achieved near the first main engine cutoff (MECO1)[13] of the trajectory and that the position error at that point was approximately 300 m. Launch vehicle position errors increased steadily after achieving the minimum value and eventually exceeded 1.6 km. The conservative approach, using the minimum launch vehicle position error and assuming it to be in the x-direction of the RMCS, resulted in a min (σ_2) of 300 m. Thus, combining these two results gives a σ_{min} of 500 m.

Selecting values of A^*.—Prior to determining a value of A^* for use in the calculation of miss distance, all space objects were divided into the following categories:

(1) Manned objects (or objects capable of being manned)
(2) Satellites (active or decommissioned)
(3) Spent rocket bodies (including platforms)
(4) Debris
(5) Uncategorized objects or objects classified for national security

A maximum area A_1 was determined for each space object category and an additional area A_2 was determined for the launch vehicle. Table I shows the areas used for each object class. The area was taken to be the products of the two largest overall dimensions. These values are based on a limited search of available data, and based on the perceived quality or quantity of the data reviewed, an adjustment factor was applied to further increase the areas.

For the portion of flight subject to the COLA analysis, the launch vehicle consisted of the Titan Stage II, the Centaur, and

---

[13]This refers to the first shutdown of the Centaur main engines that were ignited and shut down twice during the Cassini launch.

TABLE I.—MAXIMUM CROSS-SECTIONAL AREAS OF VARIOUS OBJECTS

Object class	Area, m^2
Area, A_1	
Manned objects	1100
Satellites	300
Upper stages and platforms	55
Debris	10
Uncategorized and/or classified objects	300
Area, A_2	
Launch vehicle[a]	100

[a]Consists of Titan stage II, Centaur, and the spacecraft.

TABLE II.—VALUES OF A^* BY OBJECT CLASS

Object class	Area, A^*, m^2
Manned objects	1863
Satellites	746
Upper stages and platforms	303
Debris	173
Uncategorized and/or classified objects	746

TABLE III.—REQUIRED MISS DISTANCES BASED ONLY ON PROBABILITY CALCULATIONS

Object class	Minimum miss distances, km
Manned objects	35.9
Satellites	14.4
Upper stages and platforms	5.9
Debris	3.3
Uncategorized and/or classified objects	14.4

TABLE IV.—REQUIRED MISS DISTANCES AFTER ADJUSTMENTS

Object class	Final minimum miss distances, km
Manned objects	200
Satellites	35
Upper stages and platforms	30
Debris	30
Uncategorized and/or classified objects	35

the spacecraft. The respective areas are approximately 30, 35, and 35 m^2. Even though the stages are jettisoned (Titan Stage II first and Centaur later), thereby substantially reducing the launch vehicle size, the area of the launch vehicle was conservatively taken to be 100 m^2 for the entire trajectory. Given these values of A_1 and A_2, the composite area A^* was then calculated as $A^* = \left(\sqrt{A_1} + \sqrt{A_2}\right)^2$. The resultant values of A^* are shown in table II.

Maximum allowable collision probability.—If the launch vehicle and a space object are on trajectories that result in a zero nominal miss distance, the probability of collision, using the equations derived in this report, could be as high as 10^{-4} to 10^{-3} depending on the size of the space object.

For the Cassini mission, it was desired to limit the maximum probability of collision to values less than or equal to 1.0×10^{-6}. A value of 1.0×10^{-6} is consistent with values used in other aspects of the launch approval process. However, the impact on the launch window was unacceptably large in that nearly one-half of the launch window was lost. Since the values chosen for σ_{min} and A^* are extremely conservative, it was decided that a maximum probability of 1.0×10^{-5} would be acceptable.

Computation of minimum miss distances.—The miss distance was shown in equation (36) to be

$$H^* = 0.09653 \frac{A^*}{\sigma_{min} P_C} \qquad (36)$$

Substituting the values determined in the previous section gives the miss distances, based purely on probability considerations (table III).

Adjustments to minimum miss distances.—Several adjustments were made to the computed minimum miss distances:

(1) The miss distance for manned objects was increased to 200 km to be consistent with the independent safety COLA analysis performed by the Eastern Range.

(2) Any miss distances less than 10 km were increased to 10 km.

(3) A bias of 20 km was added to all miss distances (except that for manned objects) to account for tolerances in the liftoff time.

Liftoff is nominally scheduled to occur on the whole minute. For the Cassini mission, this was subject to a tolerance of $-1, +3$ sec. To accommodate this tolerance, the COLA analysis was performed for an assumed liftoff time 1 sec after the whole minute, which (given the tolerance) meant that actual liftoff would occur ±2 s from the time analyzed. The aforementioned bias of 20 km provides a margin of safety for spacecraft traveling at a worst-case velocity of 10 km/s.

Table IV gives the final minimum required miss distances for the Cassini mission and takes into account the three adjustments and rounding the results. These miss distances assure a collision probability of less than 1.0×10^{-5}. However, given the conservatism used throughout, the actual collision probabilities are considerably less.

After finalizing these miss distances, the impact on launch window was evaluated. It was estimated that on average, 12 of 141 launch opportunities per daily launch window would be closed because of a violation of the COLA miss criteria.

Collision Avoidance Analysis Process

The miss criteria described in the previous section were established and approved several weeks before launch. Several days before launch, the trajectory generation process was initiated. The full complement of 182 daily trajectories was generated for several launch days and stored in the computer system. Approximately 48 and 24 hr prior to the planned launch, a COLA analysis was performed to identify those space objects that were most likely to come within proximity of the launch vehicle. The Air Force's 1st CACS then focused on these identified space objects to improve the orbit prediction accuracy.

Approximately 4 hr before launch, the conjunction analyzer was executed at Cheyenne Mountain Operations Center (CMOC) and simultaneously at the Naval Space Command in Dahlgren, VA. The execution time of the conjunction analyzer at CMOC was approximately 25 min.[14] The conjunction analyzer results from both organizations were compared and reviewed prior to transferring them electronically to the Eastern Range.

The Eastern Range performed the postprocessing and independently performed the safety COLA. The results of the mission assurance and safety COLA were combined and summary charts showing the unacceptable launch times were produced. After review and approval by the launch director, the charts were distributed to the appropriate launch personnel approximately 1 hr before the opening of the launch window. .

Collision Avoidance Analysis Results

Table V gives the COLA analysis results for the October 15, 1997 launch of the Cassini spacecraft. For this day, the launch window opened at 8:43 Greenwich mean time (G.m.t) and closed at 11:03, giving a launch window duration of 140 min. With launch planned to occur on the whole minute, 141 launch opportunities were provided. For the first 40 opportunities, the flight azimuth was 93°; for the next 41 opportunities, the flight azimuth could be either 93° or 97° for 82 possible trajectories; and for the last 60 opportunities, the flight azimuth was 97°. The actual liftoff time was 8:43:0.582, which was 0.582 sec later than the targeted liftoff time but well within the tolerance.

The COLA analysis identified 17 trajectories for which the preestablished miss criteria were violated. These 17 trajectories affected 14 of 141 launch opportunities. Of the 14 launch opportunities affected, 3 occurred during a time in the launch window when either a 93° or 97° launch azimuth was possible.

Each of the 17 trajectories that violated the miss criterion involved only a single conjunction with an orbiting space object that exceeded the allowable probability of collision. For each identified conjunction, table V lists some of the data of interest, including the class of object involved, the flight azimuth, the time from liftoff when the conjunction would have occurred, the predicted nominal miss distance, the flight phase, and the altitude.

TABLE V.— COLA RESULTS FOR OCTOBER 15, 1997
[Arranged chronologically with time into launch window.]

Liftoff time, G.m.t.	Object class	Flight azimuth, deg	Mission elapsed time of closest approach, s	Miss criteria, km	Nominal miss distance, km	Phase of flight[a]	Altitude of potential collision, km	Launch vehicle/ space vehicle relative velocity, km/s
8:46	Satellite	93	2250.208	35	32.2	4	639.2	11.4
8:47	Debris	93	2221.969	30	13.6	4	572.5	11.5
8:49	Debris	93	2297.930	30	17.7	4	813.6	11.3
8:54	Debris	93	2326.872	30	13.3	4	970.0	11.2
9:10	Unidentified object	93	2194.960	35	30.6	4	697.0	11.4
9:29	Satellite	93	1376.469	35	27.2	2	171.0	7.9
9:30	Debris	93	2199.076	30	5.1	4	912.7	11.3
		97	2198.463		8.7	4	914.7	11.3
9:38	Classified object	93	2195.403	35	30.8	4	988.5	11.2
		97	2194.295		27.0	4	989.9	11.2
9:44	MIR Space Station	93	1801.334	200	172.0	3	222.6	9.5
		97	1799.714		171.4	3	224.2	9.3
10:06	Debris	97	2133.053	30	27.4	4	1084.5	11.1
10:12	Satellite	97	1985.984	35	34.6	4	640.6	11.4
10:16	Rocket body	97	1306.811	30	18.3	2	170.0	7.9
10:33	Debris	97	1868.192	30	13.1	4	490.1	11.5
11:02	Satellite	97	2065.356	35	28.3	4	1473.6	10.9

[a] 1, Centaur first burn; 2, park orbit; 3, Centaur second burn; 4, between Centaur second main engine cutoff and space vehicle separation.
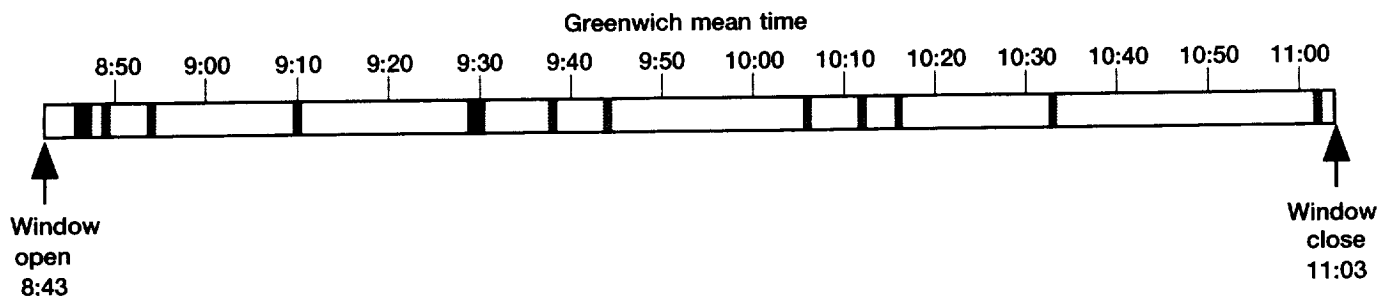
Figure 9.—October 15 Cassini launch window. Darkened areas represent times during which launch is not allowed because of risk of collision with orbiting object.

TABLE VI.— ASSUMPTIONS RELATED TO OBJECT SIZES

Object class	Area of region R^*, A^*, m²	Length of sides of rectangular region R_0^* along direction given by θ, L^*, m	Length of sides of rectangular region R_0^* along direction given by $\theta + 90°$, W^*, m
Manned Objects	1863	61.0	30.5
Satellites[a]	746	38.6	19.3
Upper stages and platforms	303	24.6	12.3
Debris	173	18.6	9.3

[a]Includes uncategorized and classified objects.

TABLE VII.—VALUES USED TO COMPUTE THE BOUND OF $|R_T|$

Terms related to maximum error	Manned objects	Satellites	Upper stages and platforms	Debris
σ_r, m	500	500	500	500
v_T, m	35 900	14 400	5900	3300
For $\rho = 0$				
λ_-, m²	1.29×10^9	2.07×10^8	3.48×10^7	1.09×10^7
λ_+, m²	2.50×10^5	2.50×10^5	2.50×10^5	2.50×10^5
A^σ, m²	5.64×10^7	2.26×10^7	9.27×10^6	5.18×10^6
For $\rho = 0.50$				
λ_-, m²	1.29×10^9	2.07×10^8	3.49×10^7	1.10×10^7
λ_+, m²	1.87×10^5	1.87×10^5	1.87×10^5	1.86×10^5
A^σ, m²	4.88×10^7	1.96×10^7	8.03×10^6	4.49×10^6
For $\rho = 0.90$				
λ_-, m²	1.29×10^9	2.08×10^8	3.50×10^7	1.11×10^7
λ_+, m²	4.75×10^4	4.75×10^4	4.72×10^4	4.66×10^4
A^σ, m²	2.46×10^7	9.86×10^6	4.04×10^6	2.26×10^6
For $\rho = 0.95$				
λ_-, m²	1.29×10^9	2.08×10^8	3.50×10^7	1.11×10^7
λ_+, m²	2.44×10^4	2.43×10^4	2.42×10^4	2.39×10^4
A^σ, m²	1.76×10^7	7.06×10^6	2.89×10^6	1.62×10^6

TABLE VIII.—UPPER BOUNDS OF $|R_T|$ FOR CASSINI

Object class	$\rho = 0$	$\rho = 0.50$	$\rho = 0.90$	$\rho = 0.95$
Manned objects	1.02×10^{-8}	1.58×10^{-8}	1.24×10^{-7}	3.37×10^{-7}
Satellites	4.10×10^{-9}	6.31×10^{-9}	4.95×10^{-8}	1.35×10^{-7}
Upper stages and platforms	1.65×10^{-9}	2.55×10^{-9}	2.00×10^{-8}	5.45×10^{-8}
Debris	9.68×10^{-10}	1.50×10^{-9}	1.18×10^{-8}	3.23×10^{-8}

Of the 17 possible conjunctions identified for an October 15 launch, 2 occurred in park orbit, 2 occurred during the Centaur second main engine burn, and the remaining 13 occurred after the second Centaur main engine cutoff (MECO2) but before spacecraft separation. In terms of altitude, the identified conjunctions occurred between 170 and 1474 km.

Figure 9 illustrates the effect of COLA closures on the launch window. The bar represents the entire 140-min launch window; the shaded areas represent lost launch opportunities due to a potential for collision with an orbiting object.

Accuracy Assessment of Cassini Probability Calculations

The miss distances established for the Cassini mission and shown in table III are based on a maximum allowable probability of collision of 1.0×10^{-5}. This section uses equation (31) to address the error in that probability value. The maximum error is a function of terms related to the covariance matrices and to terms related to the object sizes. That the object sizes affect the error term means that the error will be different for each object class. The following sections define the values used to compute the magnitude of the bound for $|R_T|$.

Assumed values for L^*, W^*, and A^*.—Table II gives the values of A^* for each object class. The values of L^* and W^* are derived by assuming somewhat arbitrarily that $L^* = 2(W^*)$. With this assumption, the values shown in table VI are obtained.

Assumed values for A^σ, λ_+, and λ_-.—Recall that the value of σ_T assumed for the Cassini analysis was 500 m. Recall also from equation (34) that the value of $v_T = v_{max} = H_{max}$. The value of H_{max} is the required miss distance given in table III. Thus, using these values of σ_T and v_T and treating the unknown

correlation parametrically yields from equation (12) the values of λ_- and λ_+ shown in table VII. (Note that the $\pm$ in equation (12) had to be reversed because v_T is greater than σ_T, as discussed in the text preceding equation (13).) Then, applying equation (29) gives the values of A^σ shown in table VII.

Computation of the upper bound for $|R_T|$.—Substituting the values from tables VI and VII into equation (31) gives the results shown in table VIII. Note that since v_T is greater than σ_T, the minor axis of the probability contour is along the direction given by θ. The dimension of the rectangular region R_0^* that is along the direction given by θ is by definition L^*. Since the orientation of the rectangle is unknown, L^* can be taken to be either the long or the short side of the rectangle. As an added measure of conservatism, the length of L^* was taken to be the larger of the two sides; thus, the long side of the region R_0^* is parallel to the minor axis of the probability density contour. This yields the largest value of $|R_T|$ bound.

All the errors shown in table VIII are with respect to a probability of collision P_C of 1.0×10^{-5}. As can be seen, under worst-case conditions, combining the largest space object with the largest value of correlation and assuming that the long side of the rectangle is at right angles to the semimajor axis of the error ellipse, the error is 3.37×10^{-7}. This represents approximately 3.4 percent of the probability of collision.

Values of the correlation of the covariance matrix Σ, which is the sum of the two independent covariance matrices of the launch vehicle and the space object, are usually not expected to be as large as 0.95. For this reason and given the large number of conservative assumptions made in the derivation of equation (31) and in the computation of the values shown in table VIII, it may be concluded that the errors in equation (9) are generally smaller than those given in the last column of table VIII.

Appendix B

Symbols

A^* area of region R^* that is a function of A_1, A_2 and the shape and orientation of the two objects

A' area of region R'

A^σ area of ellipse defined by equation $[x \quad y]\Sigma^{-1}\begin{bmatrix} x \\ y \end{bmatrix} = 1$

A_1 area of object 1 projected into x,y-plane of relative motion coordinate system (RMCS)

A_2 area of object 2 projected into x,y-plane of RMCS

D diagonal matrix, elements of which are square roots of eigenvalues of Σ

H nominal separation distance between two objects at point of closest approach

H^* value of H_{max} when $\sigma_T = \sigma_{min}$

H_{max} maximum value of H_{min} for given value of σ_T over the range of $0 \le v_{eqv} \le \infty$ (The value of H_{max} occurs when $v_{eqv} = H_{max}$.)

H_{min} minimum separation distance required to ensure that probability of collision be less than P_C for any given covariance matrix

L^* length of sides of rectangular region R_0^* along direction given by θ

L' length of sides of rectangular region R' in u-direction

M 3×3 matrix that transforms from inertial coordinates to the RMCS

N orthonormal matrix whose columns are the normalized eigenvectors of Σ and whose transpose is used to rotate R_0^*

P probability of collision of an orbiting space object with a launch vehicle and/or spacecraft

P_C probability of collision of an orbiting space object with a launch vehicle and/or spacecraft if a constant probability density function is assumed

$(P_C)_{max}$ maximum value of P_C for given value of σ_T and A^*

P_U, P_V standard normal cumulative distribution functions

p probability density function

p_C collision probability density

p_U, p_V standard normal probability density functions

R^* region of x,y-plane surrounding one object such that if center of second object is within the region, a collision will result

R' region R_0^*, after translation by $(0,-H)$, rotation by N^T, and rescaling by D^{-1}

R_0^* region R^* translated to the origin

R_T remainder term in Taylor expansion of probability of collision formula

t time

U, V standard normal random variables obtained after translation, rotation, and rescale of random variables X, Y

u, v coordinates in plane obtained after translation, rotation, and rescale of x,y-plane

u', v' coordinates of center of rectangular region R'

W^* length of sides of rectangular region R_0^* along direction given by $\theta + 90°$

W' length of sides of rectangular region R' in v-direction

X, Y, Z random variables that map trajectory event space to x-, y-, and z-values of relative location of two objects in RMCS

x, y, z coordinates in RMCS

θ angle between x-axis and semimajor (or semiminor) axis of probability contour of Σ, as well as orientation of two sides of rectangular R_0^* with respect to x-axis

λ_+, λ_- eigenvalues of Σ with λ_+ the value associated with eigenvector along direction given by θ and λ_- the value associated with eigenvector along direction given by $\theta + 90°$

v_{eqv} equivalent 1-sigma position error measured in y-direction of RMCS which, combined with a correlation of zero, would yield same probability of collision as v_T combined with ρ_T

$$\left(v_{eqv} = v_T \sqrt{1 - \rho_T^2} \right)$$

v_{max} value of v_{eqv} at which H_{min} is a maximum

v_T 1-sigma error of relative positions of object 1 and object 2 measured in y-direction of RMCS,

$$\left(v_T = \sqrt{v_1^2 + v_2^2} \right)$$

v_1 1-sigma position error of object 1 measured in y-direction of RMCS

v_2 1-sigma position error of object 2 measured in y-direction of RMCS

ρ_T correlation between σ_T and v_T

ρ_1 correlation between σ_1 and v_1

ρ_2 correlation between σ_2 and v_2

Σ 2×2 covariance matrix of marginal distribution associated with random variables X and Y, variances σ_T^2, v_T^2 and correlation ρ_T

σ_{min} minimum value of σ_T

σ_T 1-sigma error of relative positions of object 1 and object 2 measured in x-direction of RMCS

$$\left(\sigma_T = \sqrt{\sigma_1^2 + \sigma_2^2} \right)$$

σ_1 1-sigma position error of object 1 measured in x-direction of RMCS

σ_2 1-sigma position error of object 2 measured in x-direction of RMCS

$(\bullet)^T$ transpose of a matrix

$|\bullet|$ absolute value of a scalar or determinant of a matrix

$(\bullet)^{-1}$ reciprocal of a scalar or inverse of a matrix

$\ni$ such that

$\forall$ for all

References

1. Anderson, T.W.: An Introduction to Multivariate Statistical Analysis. Second ed., John Wiley & Sons, New York, NY, 1984.

2. Spiegel, M.: Mathematical Handbook of Formulas and Tables. Schaum's Outline Series, McGraw Hill, New York, NY, 1968.

3. Mood, A.M.; Graybill, F.A.; and Boes, D.C.: Introduction to the Theory of Statistics. Third ed., McGraw-Hill, New York, NY, 1974.

4. Graybill, F.A.: An Introduction to Linear Statistical Models. McGraw-Hill, New York, NY, 1961.

5. Wilkinson, J.H.: The Algebraic Eigenvalue Problem. Clarendon Press, Oxford, England, 1965.

REPORT DOCUMENTATION PAGE

Public reporting burden for this collection of information is estimated to average 1 hour per response, including the time for reviewing instructions, searching existing data sources, gathering and maintaining the data needed, and completing and reviewing the collection of information. Send comments regarding this burden estimate or any other aspect of this collection of information, including suggestions for reducing this burden, to Washington Headquarters Services, Directorate for Information Operations and Reports, 1215 Jefferson Davis Highway, Suite 1204, Arlington, VA 22202-4302, and to the Office of Management and Budget, Paperwork Reduction Project (0704-0188), Washington, DC 20503.

1. AGENCY USE ONLY (Leave blank)	2. REPORT DATE September 1999	3. REPORT TYPE AND DATES COVERED Technical Paper

4. TITLE AND SUBTITLE

Launch Collison Probability

5. FUNDING NUMBERS

WU–257–90–00–00

6. AUTHOR(S)

Gary Bollenbacher and James D. Guptill

7. PERFORMING ORGANIZATION NAME(S) AND ADDRESS(ES)

National Aeronautics and Space Administration
John H. Glenn Research Center at Lewis Field
Cleveland, Ohio 44135–3191

8. PERFORMING ORGANIZATION REPORT NUMBER

E–11468

9. SPONSORING/MONITORING AGENCY NAME(S) AND ADDRESS(ES)

National Aeronautics and Space Administration
Washington, DC 20546–0001

10. SPONSORING/MONITORING AGENCY REPORT NUMBER

NASA TP—1999-208852

11. SUPPLEMENTARY NOTES

Responsible person, Gary Bollenbacher, organization code 6250, (216) 433–2276.

12a. DISTRIBUTION/AVAILABILITY STATEMENT

Unclassified - Unlimited
Subject Categories: 15, 12 and 13   Distribution: Standard

This publication is available from the NASA Center for AeroSpace Information, (301) 621–0390.

12b. DISTRIBUTION CODE

13. ABSTRACT (Maximum 200 words)

This report analyzes the probability of a launch vehicle colliding with one of the nearly 10 000 tracked objects orbiting the Earth, given that an object on a near-collision course with the launch vehicle has been identified. Knowledge of the probability of collision throughout the launch window can be used to avoid launching at times when the probability of collision is unacceptably high. The analysis in this report assumes that the positions of the orbiting objects and the launch vehicle can be predicted as a function of time and therefore that any tracked object which comes close to the launch vehicle can be identified. The analysis further assumes that the position uncertainty of the launch vehicle and the approaching space object can be described with position covariance matrices. With these and some additional simplifying assumptions, a closed-form solution is developed using two approaches. The solution shows that the probability of collision is a function of position uncertainties, the size of the two potentially colliding objects, and the nominal separation distance at the point of closest approach. The impact of the simplifying assumptions on the accuracy of the final result is assessed and the application of the results to the Cassini mission, launched in October 1997, is described. Other factors that affect the probability of collision are also discussed. Finally, the report offers alternative approaches that can be used to evaluate the probability of collision.

14. SUBJECT TERMS

Launch; Cassini; Probability; Collision; Space debris

15. NUMBER OF PAGES
35

16. PRICE CODE
A03

17. SECURITY CLASSIFICATION OF REPORT Unclassified	18. SECURITY CLASSIFICATION OF THIS PAGE Unclassified	19. SECURITY CLASSIFICATION OF ABSTRACT Unclassified	20. LIMITATION OF ABSTRACT